THE GALAXY AND THE SOLAR SYSTEM

Roman Smoluchowski
John N. Bahcall
Mildred S. Matthews
Editors

With 34 collaborating authors

THE UNIVERSITY OF ARIZONA PRESS
TUCSON

MASS EXTINCTIONS, CRATER AGES AND COMET SHOWERS

EUGENE M. SHOEMAKER
and
RUTH F. WOLFE
U.S. Geological Survey

Six strong mass extinctions have occurred in the last ~ 250 Myr, but only three of these are accurately dated. The apparent best-fit period is 31 Myr. If mass extinctions are actually randomly distributed in time, there is about a 10% probability that the two time intervals separating the three well-dated strong extinctions would be as nearly equal as observed. The formation of large (≥ 5 km diameter) impact craters in the last 250 Myr also appears to be periodic. The period and phase of the cycles yielding the best fit to the crater ages match fairly closely the best-fit cycle obtained from strong extinctions. This apparent periodicity may also be due to chance. Sharp pulses of impact events at ~ 1 Ma and ~ 35 Ma are indicated by strewn fields of impact microspherules. These pulses coincide approximately with the last two strongest peaks in the crater-age distribution and rather precisely with two mass extinctions. The pulses are best explained by mild comet showers. Various astronomical mechanisms that have been invoked to explain periodic comet showers either are improbable or cause only weakly periodic modulation of the comet flux. The mild comet showers that appear to be recorded in the Earth's impact history probably have been produced by the nearly random close passage of stars through the Sun's comet cloud.

A now famous report by Raup and Sepkoski (1984) on the apparent periodicity of mass extinctions of families of organisms in the last 250 Ma has led to the suggestion of various astrophysical mechanisms that might produce periodic or quasi-periodic extinction of life on Earth (Davis et al. 1984; Rampino and Stothers 1984*a*; Whitmire and Jackson 1984; Schwartz and James

1984; Whitmire and Matese 1985). Most attention has been focused on the possibility that the mass extinctions were caused by impact of extraterrestrial bodies, as is suggested by considerable evidence at the Cretaceous-Tertiary boundary, about 65 Myr ago (see, e.g., Alvarez et al. 1980, 1982*a*). Accordingly, the ages of known terrestrial impact structures have been scrutinized by means of a variety of statistical tests, and are reported to be periodically distributed (Alvarez and Muller 1984; Rampino and Stothers 1984*a*; Sepkoski and Raup 1986). Periodic fluctuation in the bombardment of solid bodies has been interpreted, in turn, as the consequence of the modulation of the flux of comets in the inner solar system. This modulation might take the form of discrete pulses or "showers" of comets or of a smoother, low-amplitude variation in the comet flux.

In this chapter, we review the underlying evidence upon which the claims of periodicity of mass extinctions and crater ages have been based and compare in detail the observed geologic record of impact events on the Earth with the paleontologic record of mass extinctions. Our conclusion is that there have been pulses in the impact rate on Earth, some of which are correlated with mass extinctions, and some probably are due to comet showers. Finally, we examine briefly the efficacy or likelihood of the existence of some of the astronomical clocks purported to modulate the comet flux.

I. MASS EXTINCTIONS

Although paleontologists have tended to regard the history of changes in the biota of the Earth in terms of gradual transition (Raup 1986), there is moderately strong agreement that this history has been marked by occasional episodes of rapid loss of taxa referred to as mass extinctions (see, e.g., Newell 1967). Five or six mass-extinction events are generally acknowledged, including those near the ends of the Permian (Guadalupian and Djulfian Stages), the Triassic (Norian and Rhaetian Stages) and the Cretaceous (Maestrichtian Stage). Other, lesser extinction events have been recognized by various authors (see, e.g., Fischer and Arthur 1977). The identification and precise determination of the time and duration of mass extinctions, however, are fraught with difficulties. These difficulties arise from incompleteness in the stratigraphic record, in the record of fossils within the preserved strata, and in the study of the contained fossils—as well as from problems of global correlation of the preserved beds (see, e.g., Newell 1982; Signor and Lipps 1982; Hoffman and Ghiold 1985).

Perhaps the most exhaustive attempts to define mass extinctions on a quantitative basis have been made by Sepkoski and Raup, who used a large catalog (Sepkoski 1982*a*) of the observed stratigraphic ranges of various taxa. Working at the taxonomic level of families of organisms, Raup and Sepkoski (1982) and Sepkoski (1982*b*) reported three high- to intermediate-intensity extinctions within the last ~ 250 Myr (Djulfian, Norian and Maestrichtian

Stages) and five "lesser," possibly regional, extinctions (Toarcian, Tithonian (?), Cenomanian, late Eocene, and late Pliocene Stages). Raup and Sepkoski then expanded the list of possible mass extinctions in this ~ 250 Myr interval to include 12 events; the list formed the basis of their 1984 analysis of periodicity. Although this analysis has been superseded, to some extent, by two more recent papers (Raup and Sepkoski 1986; Sepkoski and Raup 1986), it has stimulated great interest and a number of hypotheses concerning possible astronomical driving mechanisms for extinctions. Therefore, we will review the 1984 analysis in some detail.

The extinction events recognized by Raup and Sepkoski in 1984 were found by the following procedure (1984 Raup-Sepkoski algorithm):

1. Sepkoski's catalog was screened to eliminate families whose stratigraphic range is poorly known;
2. All living families were subtracted from the screened list;
3. The number of families that are now extinct was tabulated for each stratigraphic stage (comprising 40 in all, from the Djulfian Stage of the Permian to the end of the Tertiary), and the ratio of the number of families that fail to appear in the following stage to the total number of extinct families known from each stage was used to calculate "percent extinction";
4. The time of all extinctions for each stage was plotted at the upper boundary of the stage, although the precise stratigraphic level of extinction of a given family commonly is not known, and extinctions may be distributed through a stage.

The fluctuation of "percent extinction" from one stage to the next gives rise to a series of 12 peaks (Fig. 1). Each peak found by this procedure was included in the statistical analysis for periodicity, although Raup and Sepkoski recognized explicitly that not all peaks may be significant.

Some indication of the inherent difficulty in identifying "lesser" mass extinctions is given by changes in identification by Raup and Sepkoski between 1982 and 1984. An extinction event suggested by Sepkoski (1982*b*) to occur at the end of the Toarcian Stage of the Jurassic was later resolved into two peaks, one in the Pliensbachian and the other in the Bajocian; the Toarcian extinction level, in the 1984 analysis, falls in a valley between these two peaks. The extinctions per stage at the Pliensbachian and Bajocian peaks, 15% and 11% respectively, are below the overall average level of extinction per stage from the end of the Permian to the middle Miocene (19% of extinct families per stage). A lesser mass extinction near the end of the Pliocene (at ~ 2 Ma),[a] which had been described by Stanley and Campbell (1981) and re-

[a]Ma is used here to denote the *age* of a geologic event 10^6 yr before the present. In contrast, Myr indicates the *duration* of a remote interval of time lasting 10^6 yr.

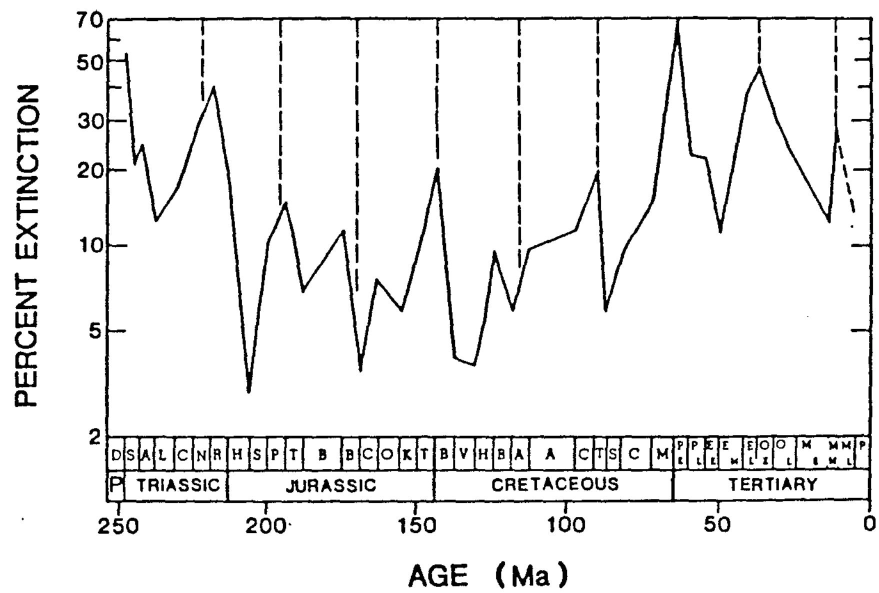

Fig. 1. Distribution of percent extinction of families with respect to time for the past 250 Myr, as calculated by the algorithm of Raup and Sepkoski (1984). Letters in small boxes along the abscissa are the stages adopted in the analysis of Raup and Sepkoski; the boundaries of the stages are plotted primarily according to the Harland et al. (1982) geologic time scale. (There is an unexplained expansion of the duration of the Bathonian in the middle of the Jurassic, as plotted by Raup and Sepkoski [1984], which does not correspond to the time scale of Harland et al. [1982].) Positions of peaks for a best-fit cycle having a 26 Myr period, determined by time series analysis by Raup and Sepkoski, are shown as dashed lines.

ported in Sepkoski's 1982 paper, was dropped in the 1984 analysis, and a peak in the middle Miocene (at 11.3 Ma according to Harland et al. [1982]) was somewhat tentatively introduced.

A peculiarity of the extinction rate calculated by the 1984 Raup-Sepkoski algorithm is that extinction rates in the relatively recent geologic past are greatly exaggerated by subtraction of living families. Families that became extinct in late Tertiary time actually constitute a very small fraction of the extinct families. The middle Miocene mass extinction, which represents a sharply defined loss of only 6 out of a total of about 700 living and extinct families was shown as questionable by Raup and Sepkoski (1984), but it has been affirmed in their later papers. The evidence cited by Sepkoski (1982*b*) for a mass extinction at the end of the Pliocene is not contravened by the 1984 analysis.

Some of the deficiencies of the 1984 Raup-Sepkoski algorithm have been rectified in their 1986 papers. First of all, percent extinction has been calculated on the basis of standing taxonomic diversity rather than on the basis of taxa now extinct. Secondly, extinction has been examined at the level of genera as well as families. The analysis at the genus level reinforces the identification of mass extinctions found to be significant at the family level. Most important, the statistical significance of the extinction peaks was examined; several of the peaks identified in the 1984 analysis have been rejected.

Among many factors that affect the apparent extinction rate are differences in the lengths of the stages (see Hoffman 1985). The durations of stages in the Late Cretaceous and Tertiary differ by as much as a factor of 3 or more; the durations of most of the stages in the Mesozoic are virtually unknown. If the actual extinction rate were perfectly uniform, it would appear to fluctuate by at least a factor of 3, and probably much more, when analyzed by the 1984 Raup-Sepkoski algorithm. Whether small peaks in the percent extinction per stage correspond to actual peaks in extinction rate cannot be determined until the apparently high rates of extinction have been verified by detailed stratigraphic studies. Peaks that lie below the average level of extinction per stage should be regarded as indicators of unusual biological events only with caution; peaks below 10% extinction per stage probably represent nothing more than statistical noise.

Sepkoski and Raup, in their 1986 paper, explicitly calculated extinction *rates* on the basis of estimated stage lengths. However, for stages older than the Albian (older than ~113 Ma) their calculated rates (25 of their total of 44 calculated rates) are virtually meaningless. In general, the uncertainties of the ages of the boundaries of the pre-Albian stages exceed the estimated durations of these stages. These uncertainties are described in detail in Harland et al. (1982, ch. 3). No pre-Albian stage duration is known within a factor of 10. We wish to stress here the inadvisability of any investigator attempting to use first derivatives of published geologic time scales without first assessing with great care the available chronometric calibration. Large errors in first derivatives are likely even for the best calibrated part of the time scale (the last 100 Myr). As an example, a duration for the late Eocene Stage of 4.0 Myr can be obtained from the ages of stage boundaries (42.0 Ma and 38.0 Ma) estimated by Harland et al. (1982), yet a more recent calibration by Montanari et al. (1985) suggests that the late Eocene lasted for only 0.7 Myr. The possible error for the duration of the late Eocene derived from Harland et al. (1982) is greater than a factor of 5.

Because the reported periodicity of Raup-Sepkoski extinction peaks was the starting point for several papers in which various astrophysical mechanisms were proposed, we review here the status and timing of each of these peaks. As the principal time scale used by Raup and Sepkoski in their 1984 and 1986 analyses is that of Harland et al. (1982), we will examine the uncertainties in this time scale as well as the inherent limits to the resolution of the time of extinctions of taxa.

Guadalupian-Djulfian Extinction (End of the Permian)

There is universal agreement that a great extinction at both the genus and family levels occurred near the end of the Permian Period. This extinction marks the change from Paleozoic to Mesozoic life. Sea level was low near the end of the Permian and beginning of the Triassic, however, so an apparently continuous record of deposition across this boundary has been found in fossiliferous rocks in only a few regions of the world. How extinctions were distributed in the Djulfian Stage (the last stage of the Permian) is not known. A major loss of taxa also took place in the preceding Guadalupian Stage of the Permian (Raup and Sepkoski 1986; Sepkoski and Raup 1986). Hence, the great terminal Paleozoic extinction was definitely distributed through at least two stages. The range of uncertainty in the estimated age of the Permian-Triassic boundary, roughly determined from chronograms presented by Harland et al. (1982), is 20 Myr. The error is not symmetrical about the 248 Ma age given for the boundary by Harland et al. (1982), which was derived by interpolation, but the age of the boundary is estimated as between about 234 and 254 Ma. The beginning of the latest Permian stage (referred to as Tartarian by Harland et al. [1982]) is also estimated to lie in this interval. Thus the interval in which the Djulfian (Tartarian) extinction is estimated to have occurred extends from 234 to 254 Ma, and the next oldest stages (referred to as Kazanian and Ufimian by Harland et al. [1982] roughly and equivalent to the Guadalupian) also fall in this interval. The great episode of extinction near the end of the Permian was distributed in an unknown way in this ~20 Myr time interval.

Olenekian Extinction

This minor extinction peak (about 2% amplitude) is on the flank of the great extinction peak near the Permian-Triassic boundary. It was recognized only by splitting the Scythian Stage and was regarded by Raup and Sepkoski (1984) as probably not significant. It has been dropped in their 1986 analyses.

Norian-Rhaetian Extinction

A major mass extinction near the end of the Triassic Period has been recognized by most specialists. Some have thought that a separate stage, the Rhaetian, should be designated in the latest Triassic, others that the Rhaetian should be included with the Norian Stage. Extinction appears highest in the Norian at the family level and highest in the Rhaetian at the genus level (Raup and Sepkoski 1986). Evidently the mass extinction is distributed over at least these two stages. The range of the estimated age of the Norian-Rhaetian boundary is from about 204 to 222 Ma (Harland et al. 1982). Both the Norian and Rhaetian Stages are estimated to range from 222 Ma or later to 204 Ma or earlier, so that the late Triassic extinction is distributed somewhere in this 18 Myr interval.

Pliensbachian, Bajocian and Callovian Extinctions

These three Jurassic extinction peaks are of low amplitude and also of very uncertain age. The Pliensbachian extinction has been accepted as significant in the 1986 Raup-Sepkoski papers and has been independently identified by biostratigraphic studies of Hallam (1976, 1977). The Bajocian and Callovian extinctions, however, have been rejected in the 1986 Raup-Sepkoski papers as not statistically significant. The end of the Bajocian is estimated to fall somewhere between 165 and 200 Ma and the end of the Pliensbachian somewhere between 167 and 199 Ma (Harland et al. 1982). The beginning and end of the Callovian fall somewhere in the interval from 150 to 165 Ma. Until the time scale for the Jurassic is improved, paleontological data for this period cannot be used for tests of periodicity of extinctions or correlation with isotopically determined crater ages.

Tithonian Extinction

This extinction at or near the end of the Jurassic is a significant mass extinction on a statistical basis and is also recognized in the detailed biostratigraphic studies of Hallam (1976, 1977). The ending date of 144 Ma for the end of the Tithonian given by the Harland et al. (1982) time scale and cited by Raup and Sepkoski was obtained by interpolation, however, and does not correspond to the best-fit age of 135 ± 3 Ma derived from reported isotopic dates (see Harland et al. 1982, ch. 3). For the beginning of the Tithonian, the best-fit age lies between 140 and 149 Ma. The Tithonian extinction probably occurred sometime between 132 and 149 Ma, most likely near the later end of this time interval.

Hauterivian Extinction

An extinction peak found by Raup and Sepkoski (1984) in the Hauterivian Stage of the Early Cretaceous rises only 3% above that in the following Barremian Stage and is no greater than the extinctions per stage in all but one of the later stages of the Cretaceous. This extinction has been found to be not statistically significant in the 1986 Raup-Sepkoski papers. Best-fit ages for the beginning and end of the Hauterivian are 124 ± 4 Ma and 122 ± 5 Ma.

Cenomanian Extinction

The time near the Cenomanian-Turonian boundary was a period of definite biological crisis, as shown not only by the Raup-Sepkoski 1984 and 1986 analyses but also by detailed biostratigraphic studies. A mass extinction occurred in five discrete steps extending from the middle late Cenomanian to the middle early Turonian (Kauffman 1984; Elder 1985; Hut et al. 1986). The following Coniacian Stage has a normal level of extinction per stage, but the stage appears to be very short (~1 Myr); the high *rate* of extinction in the Cenomanian-Turonian boundary may have continued into the Coniacian.

The end of the Cenomanian has been dated at 91.0 ± 1.5 Ma (Harland et al. 1982); the stepwise mass extinction that straddles the Cenomanian-Turonian boundary probably spanned about 2.5 Myr (Hut et al. 1986).

Maestrichtian Extinction

The disappearance of many forms of living organisms near the end of the Mesozoic Era is one of the best documented mass extinctions in the paleontological record. As summarized by Kauffman (1984), this extinction took place in about five distinct steps over a probable interval of about 2.0 to 2.5 Myr, extending from the middle-upper Maestrichtian boundary into the early Paleocene. In recent papers, the end of the Maestrichtian has been variously estimated at 65 to 66.4 Ma (Harland et al. 1982; Palmer 1983).

Late Eocene Extinction

Another well-documented stepwise mass extinction extended from latest middle Eocene to the Eocene-Oligocene boundary (Keller 1983; Corliss et al. 1984; Hut et al. 1986). According to the time scale of Harland et al. (1982) the duration of the mass extinction can be estimated at about 4 Myr, with the last step occurring at about 38 Ma. New isotopic ages presented by Montanari et al. (1985), however, indicate that the duration was only about 1 Myr and that the last step of the extinction occurred at 35.7 ± 0.4 Ma. Given the probable short duration of the late Eocene, the average rate of extinction may have been as high or higher than that of the Maestrichtian extinction.

Middle Miocene Extinction

Loss of families at this extinction peak was only about 1% of combined extinct and living families. Sepkoski and Raup (1986) showed a calculated extinction rate for the middle Miocene that appears to be much higher than average for the Tertiary, but the actual time of extinction is well defined for only half the families lost at about this time. The end of the middle Miocene is fairly accurately dated at 11 Ma.

In summary, six relatively strong mass extinctions have occurred in the last ~ 250 Myr. The last three, the Cenomanian, Maestrichtian and late Eocene, are fairly accurately dated. The range of uncertainty in timing of the three earlier strong extinctions (Guadalupian-Djulfian, Norian-Rhaetian and Tithonian) is 17 to 20 Myr. The Guadalupian-Djulfian and Norian-Rhaetian mass extinctions are separated from the poorly dated Tithonian by about 70 to 100 Myr and from the well-dated Cenomanian by about 120 to 150 Myr. Hence, they provide only relatively weak control in testing cycles fitted to the younger, well-dated extinction events.

If we choose the apparent best central values for the ages of the last four strong mass extinctions, cycles can be fitted to their ages by a least-squares procedure (Table I). If only the three relatively well-dated strong extinctions are used, the period of the best-fit cycle is fairly sharply defined at 28 Myr; the

TABLE I
Cycles Fitted to Best Estimated Ages of the Relatively Strong Mass Extinctions in the Last 250 Myr

Mass Extinction	Estimated Age (Ma)	Cycles Fitted by Least Squares					
		25-Myr Period	28-Myr Period[a]	31-Myr Period[b]	32-Myr Period[b]	33-Myr Period[b]	34-Myr Period[b]
Late Eocene	36.2[c]	38	36	35	34	32	31
Maestrichtian	65[c]	63	64	66	66	65	65
Cenomanian	91[c]	88	92	97	98	98	99
Tithonian	135[d] (132–149)	138	148	128	130	131	132
Norian-Rhaetian	204–222	213	204	221	226	197	200
Guadalupian-Djulfian	234–254	238	232	252	258	230	234

[a]Fitted only to last three comparatively well-dated strong mass extinctions.
[b]Fitted to last four strong mass extinctions, assuming the sequence from Tithonian to late Eocene is complete.
[c]Adopted best estimated age of the midpoint of stepwise mass extinction.
[d]Adopted best estimated age of the end of the Tithonian.

last peak of this fitted cycle is at 8 Ma. Extrapolation of the 28 Myr cycle back in time yields a peak at 148 Ma, close to the earliest estimated bound for the beginning of the Tithonian. Peaks are also predicted at 204 and 232 Ma, fairly close to the latest bounds estimated for the ends of the Norian and Djulfian Stages.

On the other hand, the stratigraphic studies of Hallam (1976, 1977) show that the Tithonian extinction was distributed through the Tithonian Stage (end of the Jurassic Period); if one chooses the most probable age of 135 ± 3 Ma for the end of the Tithonian from the chronogram by Harland et al. (1982) and takes this as the culmination of the distributed extinction, then the best-fit period for the last four definite mass extinctions is 32 Myr; the last predicted peak then falls at 2 Ma. This fit is based on the assumption that the sequence of four extinctions from the Tithonian to the Eocene is complete. As the residuals are fairly large, the period is not sharply defined; a 33 Myr period whose last peak is at 32 Ma is nearly as good a fit. Neither the 32 nor the 33 Myr cycles yield peaks that fall in the very broad age ranges for either the Norian-Rhaetian or Guadalupian-Djulfian mass extinctions. However, a 31 Myr cycle, whose residuals are slightly higher, predicts peaks within the age ranges of the Norian and Djulfian, and a 34 Myr cycle yields peaks at 201 and 235 Ma, which jointly fit the latest bounds for the Norian-Rhaetian and Guadalupian-Djulfian extinctions about as well as the 28 Myr cycle. Interestingly, Fischer and Arthur (1977) originally estimated the period at 32 Myr; Kitchell and Pena (1984) found a best-fit apparent periodicity of 31 Myr for the entire set of the 1984 Raup-Sepkoski extinctions of the last ~ 250 Myr and Rampino and Stothers (1984*a*) found a best-fit period of 30 Myr, from the Raup-Sepkoski extinctions.

As the Tithonian extinction evidently extended to the end of the Tithonian Stage, we find that no cycles with periods > 28 Myr fit the ages of more than four of the six strong mass extinctions particularly well. The period of the best-fit cycle for all six extinctions is 25 Myr, which is close to the 26 Myr period determined by Raup and Sepkoski (1984) and Sepkoski and Raup (1986); the 25 Myr cycle predicts a mass extinction between the Tithonian and Cenomanian, which Raup and Sepkoski (1984) identified with the low-amplitude Hauterivian peak that they have now rejected. This cycle also fits the low-amplitude middle Miocene extinction, but is out of phase with the late Pliocene extinction identified by the detailed studies of Stanley and Campbell (1981).

Because the observational base from which all the cycles listed in Table I have been derived includes, at most, six events, the case for periodicity is no longer compelling. Indeed, the evidence for periodicity rests chiefly on the relatively secure ages of just three strong mass extinctions. For a random distribution of three events over the last 91 Myr, there is about a 10% probability that the two intervals of time separating these events would be as nearly equal as observed. Kitchell and Pena (1984) calculated best-fit models for both the times and amplitudes of the 1984 Raup-Sepkoski extinctions on the assumptions of (1) a deterministic periodic impulse, (2) a deterministic cycle of sinusoidal wave form, and (3) a stochastic dynamic system. They found the stochastic model with a 31 Myr pseudocycle to provide a superior fit to the 1984 Raup-Sepkoski extinctions, taking into account the amplitudes obtained by the 1984 algorithm. In our view, this is the result that should be expected, inasmuch as the times of two-thirds of these extinctions are not known to within one-half the cycle length and, therefore, can be considered random, and the amplitudes of most of the 1984 Raup-Sepkoski extinctions depend ultimately on virtually unknown durations of the stages and can also be considered random.

II. AGES OF KNOWN TERRESTRIAL IMPACT EVENTS

If most mass extinctions are related to the impact of comets or asteroids, it is reasonable to search for correlation between the times of mass extinction and the times of known impact events. Our knowledge of the geologic record of impact events is, at present, only fragmentary, however, and the determinations of the ages of these events have diverse and, in many cases, large uncertainties. Moreover, because the geologic record of impact structures is incomplete, a well-known bias exists in the observed sample of the ages of these structures; this bias is due to a decrease in the probability of both the preservation and the discovery of impact structures with an increase in age. Iridium anomalies and strewn fields of impact glass provide additional information on the timing of large impact events that is partly independent of the recognized impact craters. In order to assess the correlation between impacts and mass extinctions, we will draw upon information both on impact structures and on these more widespread markers of impact events.

Impact Craters and Structures

In order to reduce biases in the statistics of impact crater ages due to actual losses by erosion as well as to failure to detect degraded or buried impact structures, it is useful to restrict the statistics to craters and structures above some limiting size. Most known impact craters smaller than 1 km in diameter, for example, are of late Quaternary age (Shoemaker 1983), whereas the distribution of ages of known very large impact structures is much more uniform. The discovery of structures > 20 km in diameter formed in the last 125 Myr may be nearly complete for the North American and European cratons (Grieve 1984). A compromise must be made, however, between reducing the observational bias and retaining sufficient data to obtain useful statistics; therefore, we have chosen a diameter of 5 km as the lower limiting crater size for our age distribution study. This size is somewhat above the threshold at which craters are produced by most or nearly all extraterrestrial bodies entering the atmosphere (Shoemaker 1983).

TABLE II
Impact Structures 5 km or Greater in Diameter Whose Reported or Derived Ages are 250 Myr or Less

Impact Structure	Diameter (km)	Method of Dating	Age (Ma)[a]		Reference[b]
Bosumtwi, Ghana	10.5	Fission-track	1.04 ± 0.11*		(1)
		K/Ar	1.3 ± 0.2		(2)
Zhamanshin, USSR	7	Fission-track	1.07 ± 0.05*		(1)
Elgygytgyn, USSR	19	K/Ar	3.5 ± 0.5		(3)
		Fission-track	4.5 ± 0.1*		(4)
Karla, USSR	12	Stratigraphic (late Miocene-early Pliocene)	5 ± 3		(5)
Ries, W. Germany	27	Fission-track	14.7 ± 0.4*		(1)
		K/Ar	14.8 ± 0.7		(6)
Haughton, Canada	20	Stratigraphic (Miocene)	20 ± 5		(7)
Popigai, USSR	100	Fission-track	30.5 ± 1.2*		(4)
		K/Ar	39 ± 6		(8)
Wanapitei, Canada	8.5	$^{40}Ar/^{39}Ar$	32 ± 2*		(9)
		K/Ar	37 ± 2		(10)
Mistastin, Canada	28	$^{40}Ar/^{39}Ar$	38 ± 4	mean	(11)
		K/Ar	37.8 ± 0.9	38.5 ± 2	(11)
		Fission-track	39.6 ± 4.4		(1)
Goat Paddock, Australia	5	Stratigraphic (early Eocene)	55 ± 3		(12)
Kara, USSR (includes Ust Kara)	60	K/Ar	57 ± 9		(13)
Kamensk, USSR	25	Stratigraphic (early Paleocene)	65 ± 3		(5)
Manson, USA	35	Fission-track	61 ± 18		(14)
		$^{40}Ar/^{39}Ar$	≤70*		
Lappajärvi, Finland	14	$^{40}Ar/^{39}Ar$	78 ± 2		(15)
Steen River, Canada	25	K/Ar	95 ± 7		(16)
Boltysh, USSR	25	K/Ar	88 ± 17		(17)
		Fission track	100 ± 5*		(17)
Dellen, Sweden	15	$^{40}Ar/^{39}Ar$	100 ± 2		(18)
Carswell, Canada	37	$^{40}Ar/^{39}Ar$	117 ± 8*		(18)
		K/Ar	485 ± 50		(20)
Mien, Sweden	5	Fission-track	92 ± 6		(1)
		$^{40}Ar/^{39}Ar$	119 ± 2*		(19)
Gosses Bluff, Australia	22	Fission-track	130 ± 6		(21)
		K/Ar	133 ± 3*		(21)

TABLE II (*Continued*)

Impact Structure	Diameter (km)	Method of Dating	Age (Ma)[a]	Reference[b]
Vyapryai, USSR	8	Stratigraphic (late Jurassic)	150 ± 16	(17)
Rochechouart, France	23	K/Ar	160 ± 5*	(22)
		Fission-track	198 ± 25	(1)
Puchezh-Katunki, USSR	80	K/Ar	183 ± 3	(23)
		Stratigraphic (early Bathonian)	183 ± 17	(17)
Oboloń, USSR	15	Stratigraphic (Bajocian)	183 ± 17	(24)
Manicouagan, Canada	70	K/Ar	210 ± 4 mean	(25)
		Rb/Sr	214 ± 3 212 ± 3	(26)

[a]Age dated with a precision of 20 Myr or better. Preferred age used in construction of Figs. 2 and 3 is indicated by asterisks.
[b]References: (1) Storzer and Wagner (1977); (2) Gentner et al. (1964); (3) Gurov et al. (1978); (4) Storzer and Wagner (1979); (5) Stratigraphic age from Masaitis et al. (1980). Age based on Harland et al. (1982) geologic time scale; (6) Gentner and Wagner (1969); (7) Robertson et al. (1985); (8) Masaitis et al. (1975); (9) Bottomley et al. (1979); (10) Winzer et al. (1976); (11) Mak et al. (1976); (12) Stratigraphic age from Harms et al. (1980). Age based on Harland et al. (1982) geologic time scale; (13) Masaitis et al. (1980). Although these authors cite the K/Ar age given above, they state, on the basis of regional stratigraphic evidence, that "the most probable time of formation of the crater is the interval between late Eocene and early Oligocene"; (14) Hartung et al. (1986). On the basis of the published ^{39}Ar release diagram, an age of 67.5 ± 2.5 Ma is here assigned for construction of Figs. 2 and 3; (15) Jessberger and Reimold (1980); (16) Carrigy and Short (1968); (17) Masaitis et al. (1980); (18) Bottomley (1982); (19) Bottomley et al. (1978); (20) Currie (1969); (21) Milton et al. (1972); (22) Lambert (1974); (23) Firsov (1965); (24) Val'ter et al. (1977); (25) Wolfe (1971); (26) Jahn et al. (1978).

Twenty-five terrestrial impact structures are known whose mean diameters are greater than or equal to 5 km for which ages less than 250 Myr have been reported or can be estimated with a precision thought to be better than 20 Myr (Table II). Their ages have been determined by a wide variety of methods. In many cases, measurements of age of impact glass or crystallized impact melts have been made by standard isotopic techniques, including the K/Ar, the $^{40}Ar/^{39}Ar$ plateau, and Sr/Rb methods. Some of the most precise ages have been obtained by the fission-track method. We have derived other estimates of age for several structures on the basis of stratigraphic evidence and the Harland et al. (1982) geologic time scale.

As ages have been obtained by multiple methods for 60% of the structures listed in Table II, it is instructive to compare the results obtained by different methods. One uncertainty in K/Ar dating of impact glasses or recrystallized impact melts is the degree to which old radiogenic argon was lost from the melt. These melts commonly contain unmelted clasts of older rocks that retain some preimpact argon. The inherited argon generally leads to anomalously high age estimates, particularly in very young impact glass. Most of the K/Ar ages listed for structures younger than 40 Myr old are greater than the corresponding fission-track ages, probably chiefly as a result of inherited argon. A particularly severe case is the K/Ar age of 39 ± 6 Ma listed for the Popigai structure in the Soviet Union, which has been cited in several previous studies (see, e.g., Grieve 1982; Alvarez and Muller 1984). This age is based on the average of age determinations from six different samples. A large spread of K/Ar ages was obtained from these samples, almost certainly as a consequence of inherited argon (Masaitis et al. 1975); a seventh sample yielded a much higher age. Although Soviet investigators found a fission-track age consistent with the reported mean K/Ar age (Masaitis et al. 1980), Storzer and Wagner (1979) obtained a fission-track age of only 30.5 ± 1.2 Myr, based on techniques that correct for track fading and that control other sources of error. The age found by Storzer and Wagner is close to the youngest K/Ar age obtained from Popigai impact glasses, which is probably the least affected by inherited argon. The fission-track and the youngest K/Ar ages, therefore, may be most accurate. Fission-track ages, on the other hand, are less reliable for more ancient glasses because of problems of track fading. For example, a relatively precise 119 ± 2 Myr $^{40}Ar/^{39}Ar$ plateau age reported for the Mien structure in Sweden (Table II) is more stable and is preferred to a 92 ± 6 Myr track age reported by Storzer and Wagner (1977).

Estimates of precision of the ages given in Table II are chiefly estimates of analytical precision expressed as greater than one standard deviation. For ages assigned from stratigraphic evidence, the precision listed expresses the estimated uncertainty in chronostratigraphic position, as well as the uncertainties in the calibration of the geologic time scale. The latter uncertainties are relatively small for ages < 70 Ma, but they are the dominant uncertainties for ages based on stratigraphic evidence for Jurassic and older impact structures. For almost all ages listed in Table II, the true uncertainties probably are larger than indicated by the estimated precision, owing to diverse sources of systematic error such as inherited argon, argon loss, fission-track fading, and uncertainties in the identification and the chronological range of fossil taxa. The possible hazards of systematic error, particularly in the case of K/Ar ages for impact-metamorphosed or shock-melted rocks, are indicated by the extreme difference between a relatively well-defined $^{40}Ar/^{39}Ar$ plateau age and a previously published K/Ar age for the Carswell structure, Canada (Table II).

The ages listed in Table II are portrayed graphically in Fig. 2, where the probability distribution of age for each impact structure is taken simply as a box of 2 σ width. Where more than one estimate of age is available for a given impact structure, the preferred age (indicated by asterisk in Table II) has been plotted. A somewhat more easily evaluated picture of the composite age probability distribution is obtained by smoothing the distribution of Fig. 2 with a 6-Myr running mean (Fig. 3). Because of the unknown magnitude of the systematic errors, it does not appear that a more sophisticated representation

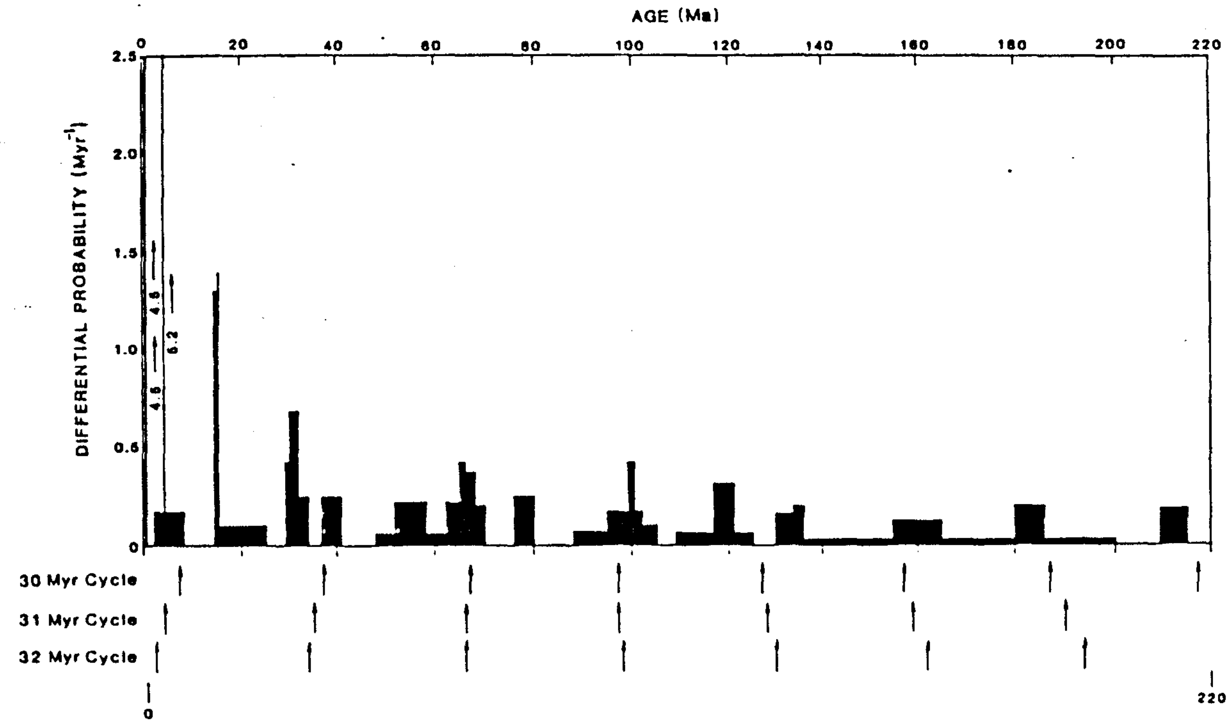

Fig. 2. Probability distribution of ages of known impact structures ⩾ 5 km in diameter for which ages of < 250 Myr have been reported or can be estimated with a precision thought to be better than 20 Myr. The probability distribution of age for each dated structure is taken as a box of 2 σ width, and the probabilities are summed where they overlap. Positions of the maxima of 30, 31 and 32 Myr cycles fitted to the observed distribution of ages are shown below the plot of the probability distribution. The 30 and 31 Myr cycles fit the entire distribution of ages equally well. The 31-Myr cycle best fits the distribution observed for the last 165 Myr, and the 32 Myr cycle best fits the distribution observed for the last 100 Myr.

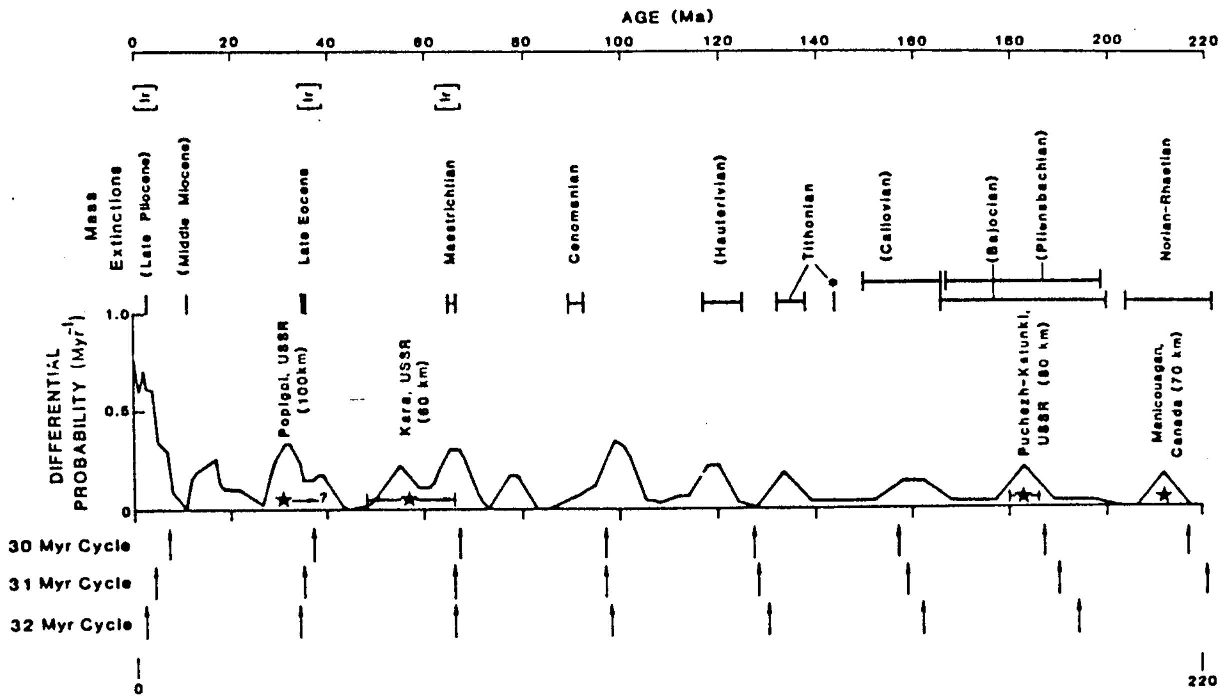

Fig. 3. Probability distribution of ages of known impact structures compared with the times of mass extinctions for the last 220 Myr. In this figure, the probability distribution of ages shown in Fig. 2 has been smoothed with a 6 Myr running mean in order to facilitate comparison with times of mass extinction. Best-fit 30, 31 and 32 Myr cycles are shown below the distribution of ages, as in Fig. 2. Isotopically determined ages of the four largest known impact structures formed during the last 220 Myr are shown with stars. The range of uncertainty of the time of each mass extinction recognized by Raup and Sepkoski (1984) is shown by error bars above the probability distribution of ages of impact structures. These times are derived from the geologic time scale of Harland et al. (1982). Weak to moderate and questionable mass extinctions are indicated in parentheses (see text). A mass extinction in the late Pliocene reported by Stanley and Campbell (1981) and recognized by Sepkoski (1982) is also shown. Two times are shown for the Tithonian mass extinction: (1) the range of uncertainty of the end of the Tithonian obtained from the chronogram of Harland et al. (1982); and (2) the age (shown with *) of the end of the Tithonian obtained by linear interpolation between chronometric tie points at 113 and 238 Ma.

of the data (such as modeling the probability distributions of age for individual structures with Gaussian functions, as was done by Alvarez and Muller [1984]) is warranted.

Inspection of Figs. 2 and 3 and Table II reveals that the number of relatively well-dated impact structures decreases with increasing age, as expected from known observational and geologic selection effects. The total number of dated structures listed in Table II decreases, on average, by about 44% in each successive interval of 75 Myr. When the decrease is fit to an exponential function, the number decreases by half per 90 Myr increase in age (characteristic time for decrease is 130 Myr). Of course, the structures listed are only a fraction of the known impact structures younger than 250 Myr. At least 16 other impact structures greater than 5 km in diameter are known whose ages probably lie in this interval but whose dates do not yet meet our rather broad precision limits. A plot of the cumulative size-frequency distribution for the impact structures with ages in the intervals 0–75 Ma, 75–150 Ma, and 150–225 Ma (Fig. 4) shows that the decrease in the number of recognized structures with increase in age applies chiefly to structures < 50 km in diameter. As many craters > 50 km in diameter are recognized in the 150–225 Ma age range as in the 0–75 Ma age range, although none this size has yet been dated in the age range 75–150 Ma (log 50 ≃ 1.7).

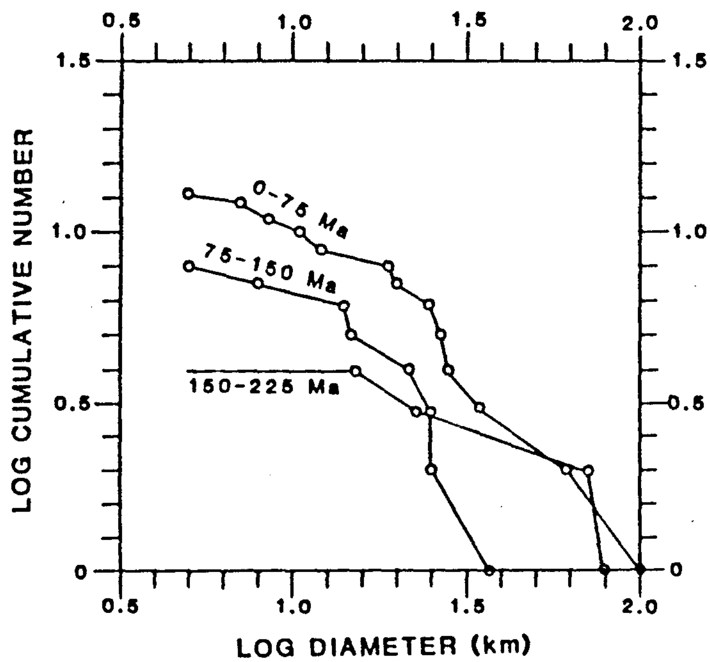

Fig. 4. Size-frequency distribution of dated terrestrial impact structures ⩾ 5 km in diameter in the age ranges 0 to 75, 75 to 150 and 150 to 225 Ma.

The probability distribution of observed ages shown in Fig. 3 consists of a pattern of peaks somewhat irregularly distributed over the past 220 Myr. Many of the peaks correspond to relatively precise individual ages; for the most part, the occurrence of these peaks is simply a reflection of the low density of age data in the time interval investigated. Four peaks, centered at about 2, 32, 65 and 99 Ma, rise above the rest of the peaks shown in Fig. 3. Each represents a cluster of three or more ages. This type of clustering resembles that generally found in random time sequences of events commonly referred to as "shot noise." Most distributions of 25 ages drawn at random from a uniformly distributed population of ages will contain several similar clusters. Hence, the presence of these peaks does not, by itself, indicate surges or modulation of the underlying cratering rate.

The highest peak shown in Fig. 3, which is centered at about 2 Ma, represents four impact events in the last 8 Myr, at least three of which occurred within a 4 Myr interval. There is about a 29% probability that three precisely determined ages out of 25 that are randomly distributed over 225 Myr would fall in the last 4 Myr and about a 4% chance that a fourth age would also fall in this interval. However, with a characteristic time of 130 Myr for the decrease in average probability of observing ages of impact structures, ages are expected to be observed about 5.5 times more frequently near the present than at 225 Ma, and twice as frequently at the present as at 90 Ma. After correction for the selection effects, even the strongest peak in the observed crater-age distribution is not statistically significant at the 95% confidence level. There is about a 50% chance that four crater ages drawn from 25 ages distributed randomly over 225 Myr would fall in a cluster spanning only 4 Myr.

Our primary purpose here is to test whether the ages of impact structures are correlated with mass extinctions. This question is partly independent of the tests for random or periodic surges in the cratering rate. Mass extinctions might arise from single large impact events or from real randomly occurring clusters of large impacts. Single observed ages of impact structures may also be samples of age clusters, particularly at times earlier than 100 Ma, as our knowledge of the actual cratering history is especially incomplete for these times.

In Fig. 3, one can see a moderate correlation between the relatively accurately dated mass extinctions in the last 100 Myr and the four strongest peaks in the probability distribution of crater ages. The stepwise mass extinction spanning the Cretaceous-Tertiary boundary is centered on the crater-age peak at $\sim$ 65 Ma, and the late Eocene stepwise mass extinction occurs on the shoulder of the $\sim$ 32 Ma crater-age peak. The precise position of the $\sim$ 32 Ma peak is uncertain, owing to the problem of interpreting the age of the Popigai crater; the true peak of crater ages might be closer to the Eocene mass extinction than shown.

Two of the four largest known impact structures of Phanerozoic age may be associated with the ~ 32 Ma and ~ 65 Ma peaks. Within the uncertainty of the K/Ar age determination, the 60 km diameter Kara crater might be correlated with the Cretaceous-Tertiary mass extinction. On the other hand, if the stratigraphic age assignment given by Masaitis et al. (1980) is correct (see footnotes to Table II), the Kara crater, along with the 100 km diameter Popigai crater, might be associated with the late Eocene mass extinction. As described below, iridium anomalies and other stratigraphic tracers of large impact events are precisely correlated with individual extinctions at the Cretaceous-Tertiary boundary and in the late Eocene. Hence, these extinctions are unequivocally correlated in time with large impact events, and the observed crater-age peaks at or near these times probably reflect or are at least close in time to real surges in the cratering rate.

The Pliocene mass extinction reported by Stanley and Campbell (1981) and by Sepkoski (1982*b*) is centered on the ~ 2 Ma crater-age peak. Although Sepkoski considered this extinction to be only regional, and although it was not included in the 1984 Raup-Sepkoski mass extinction list, it is fairly closely associated in time with a number of known impact events, including at least one major event, as shown below. Curiously, a local iridium anomaly has been discovered in late Pliocene deep-sea sediments (age ~ 2.3 Ma) near Antarctica (Crocket and Kuo 1979; Kyte et al. 1981); the anomaly is very close in age but apparently slightly younger than a significant extinction of radiolarian species that is estimated by Hays and Opdyke (1967) to have occurred at ~ 2.5 Ma. The anomaly is associated with definite meteoritic particles (Kyte and Brownlee 1985), and it is considered to have been produced by impact in the ocean of a basaltic asteroid 100 to 500 m in diameter. This event may be merely part of the background-level asteroid bombardment of the Earth, but it is intriguing that it occurred during an apparent surge in the impact rate that is fairly closely correlated with the late Pliocene extinction (see below).

Two Raup-Sepkoski extinction events in the last 100 Myr do not correlate well with crater-age peaks. The relatively weak mass extinction in the middle Miocene, if it occurred at the end of the middle Miocene, as assumed by Raup and Sepkoski (1984,1986), is about 3.5 Myr younger than the accurately dated Ries crater in West Germany and the correlative tektite (moldavite) strewn field and of the order of 10 Myr younger than the Haughton crater of early Miocene age in Canada. In any case, there is neither a strongly defined crater-age peak nor a strong mass extinction late in the middle Miocene.

The strong and relatively accurately dated stepwise mass extinction spanning the Cenomanian-Turonian boundary does not coincide with a crater-age peak; the nearest is the ~ 99 Ma peak, which is offset from the center of the extinction by about 8 Myr. This appears to be a clear miss, although the relatively poorly dated Boltysh structure in the USSR, as well as the Steen River structure in Canada, might have been formed at about the time of the Cenomanian-Turonian boundary. No iridium anomalies or other stratigraphic tracers of large impacts have yet been found at any of the Cenomanian-Turonian extinction steps, despite searches for them and a false report of an iridium anomaly (see Hut et al. 1986). There is no strong evidence that links the Cenomanian-Turonian extinction to impacts.

The dating of mass extinctions older than 100 Myr is so uncertain that, in most cases, detailed comparison of the timing of these events with crater-age peaks older than 100 Myr cannot be made. However, a crater-age peak occurs within the possible time range of each of the six Raup-Sepkoski extinctions identified between ~ 100 and 225 Ma. Each of these peaks corresponds to a single age determined with relatively high precision. No precise crater ages are available for the time between 225 Ma and 254 Ma (the earliest likely time of the Permian-Triassic boundary), although the age of the 23-km-diameter St. Martin structure of Canada, cited by Grieve et al. (1985) to be at 225 ± 25 Ma, probably falls in this interval. It is of interest that the age of one of the largest known Phanerozoic (i.e., the Paleozoic, Mesozoic and Cenozoic eras taken together) impact structures (Manicouagan, Canada) is nearly centered in the estimated range of possible age of the strong Norian-Rhaetian mass extinction.

Three of the mass extinctions older than 100 Myr shown in Fig. 3 (Bajocian, Callovian and Hauterivian) are not considered to be statistically significant, as described above. However, the age of the Puchezh-Katunki structure in the USSR is estimated from stratigraphic evidence to be early Bathonian (Table II). This great impact event could have coincided with the possible extinction event placed by Raup and Sepkoski at the end of the Bajocian (11% extinction). The 15 km diameter Obolon' structure in the USSR, estimated from the stratigraphic evidence to be of Bajocian age (Table II), might be contemporaneous with the tentative Bajocian extinction, if the Bajocian extinction preceded the end of the Bajocian Stage.

As a number of claims have been made concerning the periodicity of the ages of impact structures, it is pertinent to reexamine these claims on the basis of our updated list of ages presented in Table II. Following procedures of least-squares fitting similar to those employed by Rampino and Stothers (1984*a*), one can find best-fit cycles for the entire sequence of ages given in Table II or for various parts of it. A choice can be made either to rigidly fit a cycle to the entire sequence, which extends to 212 ± 3 Ma, or to consider the period somewhat variable, so that fits can be made to different parts of the sequence. Here we examine several cases.

For the entire sequence of 25 ages, periods of 30 and 31 Myr fit equally well; the last maxima in the cratering rate fall at 7 and 4 Ma, respectively. The mean squared deviation of observed ages from the idealized 30 and 31 Myr cycles is 55% of that expected for purely random distributions of age. Hence, there is a suggestion of periodicity in the distribution of crater ages, but there is also clear evidence of a strong nonperiodic component. If we consider ages that extend to only 165 Ma, which include 84% of the observations, the best-fit period is 31 Myr, but a 32 Myr cycle fits almost as well, with the time of its last maximum falling at 2 Ma. The mean squared deviations of the observed ages for these fits are 54% and 56% of that expected for random distributions. If one considers only the last 100 Myr interval, which includes 68% of the observations, the best-fit cycle is sharply defined with a period of 32 Myr.

The four highest peaks in the probability distribution of crater ages appear fairly strongly periodic. However, a number of accurately determined ages in the last 100 Myr interval are well separated from these peaks. If the crater-age clusters are periodic, an unequivocal second component exists that is probably random. The distribution of the various best-fit cycles is illustrated in Fig. 3. The period and phase of the best-fit cycle to the crater ages for the last 100 Myr match those of the best-fit cycle for the last four strong mass extinctions, when fitted with the assumption that the sequence of these four mass extinctions is complete.

The statistical significance of the apparent periodicity of the crater ages remains open to question. Grieve et al. (1985), using a list of 26 crater ages that is similar but not identical with ours, tested for periodicity by time-series analysis. On the basis of various criteria of data selection, they found periods of ~ 29, ~ 21, ~ 18.5 and ~ 13.5 Myr, with diverse power and phase. They also found that periodicities equivalent in power to those determined from the observed ages could be obtained in about 25% of their Monte Carlo runs when sets of 20 random numbers chosen from 1 to 250 were used. The apparent periodicity of the crater ages, considered by themselves, probably is not significant at the 95% confidence level.

Impact Glasses, Microspherules and Iridium Anomalies

Widely dispersed glass, produced by shock melting of rock, and iridium anomalies detected at discrete horizons in the stratigraphic column constitute an important record of impact events in the last 65 Myr. This record supplements the evidence from impact craters (Table III). At least 12 and possibly 13 impact events in the past 65 Myr can be identified from strewn fields of tektites, from microtektites and related glassy or cryptocrystalline microspherules, from other impact glasses, such as Libyan desert glass and Darwin glass, and from iridium anomalies discovered in sediments of late Pliocene and late Eocene age and in a thin claystone at the Cretaceous-Tertiary boundary. For five of these events, the associated or apparently associated impact crater has been identified; however, only three of these craters—Zhamanshin, Bosumtwi and Ries—are independently dated and listed in Table II. One of the associated craters, the Darwin crater, is smaller than our 5-km-diameter cutoff; the Darwin glass strewn field evidently records a relatively minor impact event. On the other hand, impacts that produced very widely distributed microspherules associated with an iridium anomaly in the late Eocene, and microspherules, shocked mineral grains and the associated iridium anomaly in

TABLE III
Ages of Strewn Fields of Impact Glass and Stratigraphic Iridium Anomalies

	Method of Dating	Age (Ma)	Reference[f]
Indochinites and philippinites	$^{40}Ar/^{39}Ar$	0.690 ± 0.028	(1)
(includes microtektites)	Fission-track	0.693 ± 0.025	(2)
Darwin glass[a]	K/Ar	0.70 ± 0.08	
	Fission-track	0.74 ± 0.04	(3)
Australites	Fission-track	0.830 ± 0.028	(2)
	K/Ar	0.86 ± 0.06	(4)
	$^{40}Ar/^{39}Ar$	0.887 ± 0.034	(1)
Irgizites[b]	Fission-track	1.07 ± 0.06	(5)
Ivory Coast tektites[c] (includes microtektites)	Fission-track	1.08 ± 0.10	(6)
Iridium anomaly and meteoritic particles in late Pliocene deep-sea sediments	Stratigraphic	2.3 ± 0.1	(7)
South Australian high-Na tektites	Fission-track	≥8.35 ± 0.90	(8)
Moldavites[d]	Fission-track	14.7 ± 0.4	(6)
Libyan Desert glass[e]	Fission-track	29.4 ± 0.5	(6)
North American tektites	Fission-track	34.6 ± 0.7	(6)
(includes microtektites)	Stratigraphic	36.0 ± 0.5	(9)
Clinopyroxene-bearing spherules and microtektites in *Globorotalia cerroazulensis* zone. Associated with strong iridium anomaly	Stratigraphic	36.0 ± 0.5	(9)
Cryptocrystalline spherules and microtektites in *Globigerapsis semiinvoluta* zone	Stratigraphic	36.4 ± 0.5	(9)
Iridium-bearing clay layer at Cretaceous-Tertiary boundary containing microspherules of diverse mineral composition and shocked grains of quartz and feldspar	Stratigraphic	65.0 ± 1.0	(10)

[a]Associated with "Darwin" crater, Tasmania (undated).
[b]Associated with Zhamanshin crater, USSR.
[c]Associated with Bosumtwi crater, Ghana.
[d]Associated with Ries crater, W. Germany.
[e]Apparently associated with Oasis crater, Libya (undated).
[f]References: (1) Storzer et al. (1984); (2) Storzer and Wagner (1980); (3) Gentner et al. (1973); (4) McDougall and Lovering (1969); (5) Storzer and Wagner (1979); (6) Storzer and Wagner (1977); (7) Age determined from paleontology and magnetostratigraphy of deep-sea core (Hays and Opdyke 1967); (8) Storzer (1985); (9) Age assigned on the basis of stratigraphic position and a new K/Ar–Sr/Rb calibration of the geologic time scale in the late Eocene by Montanari et al. (1985); (10) Age assigned from Harland et al. (1982) geologic time scale.

the Cretaceous-Tertiary boundary claystone may have released more kinetic energy than any of the impacts that formed the largest known Phanerozoic craters.

Most ages of impact events recognized from the sources of evidence listed in Table III are grouped into two well-defined clusters, one centered at about 35 Ma and the other at about 1 Ma. These clusters correspond fairly closely to the two youngest peaks recognized from the distribution of crater ages. If ages of impact glasses that are derived from well-dated craters are eliminated, four ages remain in the ~ 35 Ma cluster and four in the 1 Ma cluster. These clusters represent a set of observations that are completely independent of crater-age data. Only two of the remaining ages in Table III fall outside these clusters, one at the Cretaceous-Tertiary boundary and one in the late Miocene. The Cretaceous-Tertiary boundary event falls on the ~ 65 Ma crater-age peak. Hence, in the last 65 Myr, the ages of nearly all impact events recognized from the independent evidence of impact glass, microspherules and iridium anomalies are correlated closely with the three principal peaks observed in the crater-age distribution.

The relations of the best-fit cycles derived from the crater ages to the ages of tektites and related glass, the microtektites and related spherules, and the known associated iridium anomalies are shown in Fig. 5. Two cycles derived from the crater ages fit the ages in Table III rather well: the 31 Myr cycle, whose last maximum was 4 Ma, and the 32 Myr cycle whose last

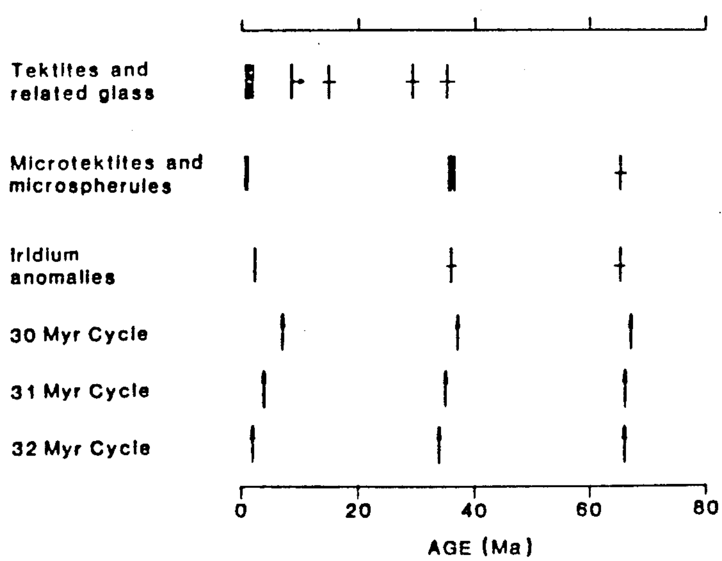

Fig. 5. Age distribution of impact events recorded by tektites and related glass, by microtektites and microspherules, and by iridium anomalies in the stratigraphic column. Uncertainties in the ages are indicated by horizontal bars. Cycles fitted to the distribution of ages of known impact structures are also shown.

maximum was at 2 Ma. In fact, the best-fit cycle derived directly from the ages of Table III has a period of 31 Myr and the last maximum was at 4 Ma; observed ages depart from a 32 Myr cycle whose last maximum was at 3 Ma with only a slightly higher mean squared deviation. The mean squared deviations of the entire set of ages from the 31 and 32 Myr cycles are $< 25\%$ of those expected for a random distribution; for the 31 Myr cycle, the mean squared deviation of ages of only the microspherules and iridium anomalies is $< 10\%$ of that expected for a random distribution. Thus, the apparent periodicity found in the distribution of crater ages over the last 165 Myr is reflected much more strongly in the ages of impact glass and iridium anomalies in the last 65 Myr.

The distribution of microspherules and iridium anomalies in the stratigraphic column permits a much more precise test of the time relation between impacts and mass extinctions than does the distribution of crater ages. The Cretaceous-Tertiary boundary claystone that contains anomalous abundances of iridium and other noble metals, as well as microspherules and shocked mineral grains has now been identified in the stratigraphic section at about 70 sites around the world. It coincides with the most thoroughly studied and documented extinction in the entire stratigraphic record. This extinction event marking the end of the Cretaceous (end of the Maestrichtian stage) is only one, perhaps the most severe of about five sharp extinctions that occurred in an interval of a few million years, however, and a search for evidence of major impacts at the times of the other extinction steps should be undertaken.

Three horizons of microtektites and microspherules in late Eocene strata lie within the stratigraphic sequence spanned by the late Eocene stepwise mass extinction. One of these microspherule horizons in the *Globorotalia cerroazulensis* foraminiferal zone, which coincides with a relatively strong iridium anomaly (Table III), is correlated with an extinction of radiolaria (Hut et al. 1986). This microspherule horizon and associated iridium anomaly have been identified over a very large area extending from the Carribean to the central Pacific; they clearly record a major impact event, possibly one that produced a large, as yet undiscovered, crater in the sea floor. The stratigraphic distribution of radiolaria in the late Eocene is best defined in sections on Barbados, where the iridium anomaly is found to coincide with a sharply defined extinction of about 25% of the identified extant radiolarian taxa (Sanfillipo et al. 1985). At these sites, the microsperules associated with the iridium anomaly have been almost entirely lost by solution corrosion (Hut et al. 1986), but they are well preserved in deep sea cores obtained in the Caribbean and Gulf of Mexico (Glass 1986).

In the Caribbean and Gulf of Mexico, a microtektite horizon that is correlated with the North American tektites occurs a few tens of centimeters above the stratigraphic position of the iridium anomaly (Glass et al. 1982; Glass et al. 1985). No extinctions have been recognized at the North American microtektite horizon, but here the foraminifera show evidence of environmental stress (Hut et al. 1986; Keller et al. 1986).

The stratigraphically lowest microspherule horizon of late Eocene age is found in the *Globigerapsis semiinvoluta* foraminiferal zone (Table III). It coincides with an episode of strong environmental stress marked by an abrupt permanent decline of the *Globigerapsis* group from about 50% to 1% of the planktonic foraminiferal faunas (Hut et al. 1986; Keller 1983; Keller et al. 1985,1986). As noted by Hut et al. (1986) and Keller (1986), the time of extinction of species is not necessarily the best indicator of environmental stress, as species commonly are rare at the time of their final demise, which may occur as a result of minor ecological perturbations. Hence, the impact-induced environmental crises in the late Eocene may be closely related to the observed stepwise mass extinction of the late Eocene, even though the microspherule horizons do not, in every case, coincide with the extinction steps. Several of these steps do coincide with abrupt cooling events in the ocean (Keller et al. 1983), which conceivably could have been triggered by major impacts not yet recognized.

In this context, it is of interest that the ~ 2 Ma crater-age peak and associated tektite- and microtektite-producing impact events occurred at about the time of a major change in global climate near the end of the Pliocene that resulted in the great Pleistocene glaciations. In all likelihood, the late Pliocene mass extinction was related to this climate change (Stanley 1984), but it is pertinent to ask whether the late Pliocene-Pleistocene glaciations were, themselves, brought about by the apparent surge in the impact rate. Discrete short cooling events caused by global veils of dust from large impacts might have been responsible for the inception of major continental glaciation, provided that the pattern of oceanic circulation in the already cool ocean and an existing ice sheet in Antarctica had set the stage. Many large impacts occurred during the Pleistocene, including at least one that produced a widespread microtektite horizon in the Indian Ocean correlative with Southeast Asian tektites (Table III). An extinction of one radiolarian species at the time of the Jaramillo magnetic event at 1.0 Ma (Hays 1971) appears to be nearly coincident with the formation of the Zhamanshin and Bosumtwi craters and the strewn field of Ivory Coast tektites and microtektites associated with Bosumtwi.

In summary, there is clear-cut evidence of a broad correlation in time between apparent pulses in the impact rate and the major stepwise mass extinctions near the Cretaceous-Tertiary boundary and in the late Eocene. Specific extinction steps in each of these stepwise mass extinctions are coincident with major impact events. Not all recognized impact events are precisely correlated with extinction steps, however. Circumstantial evidence suggests that the ~ 2 Ma peak in the cratering rate may be related to late Pliocene-Pleistocene continental glaciation and to the late Pliocene mass extinction. Episodes of relatively frequent impact-induced global environmental crises may have been more effective in producing mass extinctions than individual very large impact events. Moreover, multiple large impacts and an accompanying increase in the infall rate of cometary dust may have caused climatic instability or may have triggered long-lasting climate changes, and thereby led indirectly to mass extinctions. Hence, not all extinction steps in a time-extended mass extinction should necessarily coincide with large impact events, even if a surge in the impact rate is the ultimate or a contributing cause.

III. EVIDENCE FOR COMET SHOWERS

The combined data on ages of craters and strewn fields of impact glass and associated iridium anomalies indicate at least three and possibly four pulses or surges in the terrestrial impact rate in the last 100 Myr. These surges might be due to a variety of causes. First of all, some of the largest and comparatively rare impact events should have occurred in random clusters in time. This type of surge, which is a perfectly real phenomenon (as opposed to an apparent surge due to sampling error), may be thought of as true "shot noise" in the impact history. The surge of large impacts would not be expected to be accompanied by a surge in the much more numerous small impact events, however, and should not show up in statistics based chiefly on relatively small craters (i.e., craters < 20 km diameter). Thus, the ~ 2 and ~ 99 Ma crater-age peaks are unlikely to represent surges of this type, but, on the basis of crater ages alone, the ~ 32 and ~ 65 Ma peaks might be examples of "shot noise" surges.

Secondly, a surge in the impact rate on Earth can be produced by catastrophic collisional breakup of a large (100 to 200 km diameter) asteroid in the main asteroid belt (Shoemaker 1984*b*). Depending on the position of the asteroid in orbital element phase space, collision fragments can be delivered to one or more resonances and subsequently perturbed to Earth-crossing orbits. Appreciable surges due to breakup of large asteroids should occur once every few hundred million years, and they can be expected to have a characteristic decay time of a few tens of million years (Shoemaker 1984*b*). The ~ 65 Ma crater-age peak, or perhaps the ~ 99 Ma peak, could be related to surges of this type.

A third type of surge expected in the Earth's cratering history is produced by a shower of comets caused by close passage of a star through the comet cloud that surrounds the Sun (Hills 1981). The strength of this type of surge depends on the mass, velocity and impact parameter (miss distance) of the star relative to the Sun and on the space density and distribution of comets in a theoretical inner reservoir of comets, where comet semimajor axes range between about 500 and 10,000 AU. As there are both theoretical and fairly strong empirical grounds to infer a fairly massive inner cloud or reservoir of comets (Shoemaker and Wolfe 1984; chapter by Weissman), there are good reasons to think that comet showers have, in fact, occurred. Hills (1981) calculated that very strong comet showers ($\sim 10^4$ comets passing perihelion per year) have a frequency of about once per 500 Myr. On the basis of a theoretical model of the inner comet cloud (Shoemaker and Wolfe 1984, and unpublished analysis) and the present observed flux of stars in the solar neighborhood, we calculate that significant, but much milder, comet showers occur as frequently as once every few tens of million years, on average. All four of the observed crater-age peaks of the last 100 Myr might reflect comparatively mild comet showers.

A critical test for surges in the cratering record due to comet showers is the decay time of the surges. Comets injected by stellar perturbation into Earth-crossing orbits are fairly quickly ejected from the solar system by planetary perturbations, chiefly those of Jupiter. The characteristic decay time for comet showers produced by stellar perturbations has been found from very extensive Monte Carlo simulations to be close to 1 Myr (Hut et al. 1986). If the perturbation is due to a relatively distant passage of a giant molecular cloud, the duration of the comet shower may be extended for about 1 Myr more. For simplicity of calculation, we will adopt a half-life of 1 Myr as reasonably representative of the decay of comet showers.

If comet showers are periodic, one can calculate the cumulative frequency distributions of deviations of ages of the dated impact structures listed in Table II from the various best-fit cycles (Fig. 6). The observed distributions of deviations of age from the 30, 31 and 32 Myr cycles lie, on average, about midway between the theoretical distribution (1 Myr half-life) for comet showers and for purely random distributions of age. The distribution of deviations from the 32 Myr cycle is closest to that predicted for comet showers, up to about 50% cumulative frequency, but the remainder of the distribution approaches that expected for randomly distributed ages. In part, this approach to the random distribution line reflects the fact that the apparent 32 Myr periodicity is best defined for the last 100 Myr and tends to break down in the time interval of 100 Ma to 225 Ma.

A better fit to the theoretical distribution for comet showers can be obtained if the time interval between showers is considered to be somewhat variable, but, even with the most flexible fits that maintain the 30, 31 and 32 Myr average periods, the "random" component remains at the level of several tens of percent. Of course, some of the deviations could be due to error of age determination, but it should be borne in mind that the cycles have been fitted to the observations. In this type of comparison, therefore, perfectly random distributions of 25 ages tend to be biased away from the random-distribution lines shown in Fig. 6. Within the observational errors of age determination, it appears plausible that at least half of the relatively precisely dated impact structures could be associated with quasi-periodic comet showers.

Given the errors of age determination, identification of impact surges due to comet showers must rest, in the final analysis, on clusters of dated impact events that have the highest relative precision. In general, only the ages of

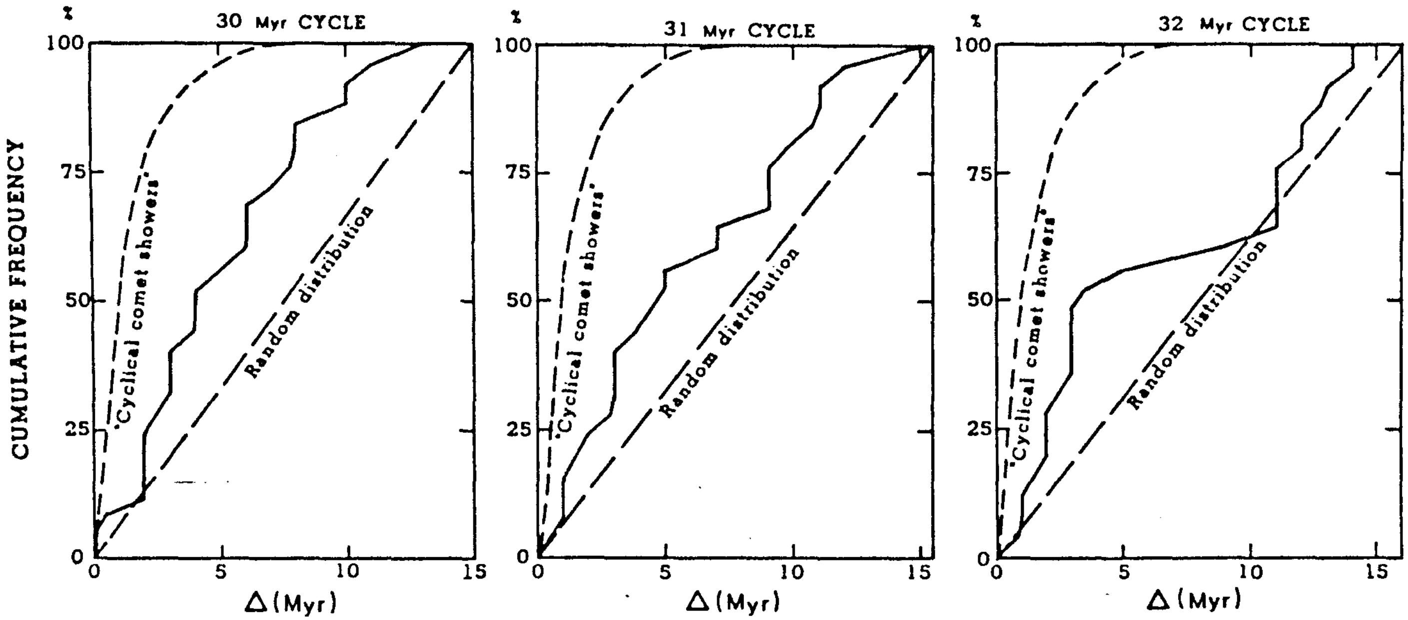

Fig. 6. Frequency distributions of the deviations of ages (Δ Myr) of known impact structures from the best-fit 30, 31 and 32 Myr cycles. Deviations of observed ages for structures ≥ 5 km in diameter formed in the last 250 Myr are shown; only ages determined with a precision better than 20 Myr have been included. For comparison, the cumulative frequency of deviations for perfectly periodic comet showers with 1 Myr half lives and for random distributions are also shown.

craters formed in the last 15 Myr and the relative ages of impact glass horizons in deep-sea sediments are dated with a precision better than 1 Myr; only these ages provide strong tests for the comet shower hypothesis. In this regard, the clustering of ages of known microtektites and other glassy microspherules into two tight groups at ~ 1 Ma and ~ 35 Ma is a striking observational result. In each cluster, the spread of ages is less than the probable duration of comet showers.

The stratigraphic spacing of two microspherule horizons in the upper Eocene, in particular, appears indicative of a comet shower. The spherule-bearing layers are so close, in fact, that at one stage of investigation they were thought to be at the same stratigraphic horizon (see, e.g., Glass et al. 1979). After discovery of an iridium anomaly just below the North American microtektite horizon in a deep-sea core in the Caribbean (Ganapathy 1982), a reexamination of the core revealed a second horizon of chemically distinct microspherules, many of which are crystal bearing, that is coincident with the iridium anomaly. This lower spherule horizon and the associated iridium anomaly have proven to be areally much more extensive than the North American microtektites (Glass et al. 1985). The geographic distributions of the two horizons overlap in the Caribbean region and Gulf of Mexico. On the assumption that average rates of sedimentation during the late Eocene apply to the ~30 cm of clay that separates the two horizons, the time interval between deposition of the two spherule layers has been estimated to be as short as 13,000 to 14,000 yr (Sanfilippo et al. 1985). The clay separating the two spherule horizons has a very low carbonate content everywhere, however, due either to leaching of carbonate or to low biological productivity, either of which may be the consequence of an impact-induced environmental crisis. Thus, the actual time interval represented by the ~ 30 cm of sediments between the two horizons is not precisely known. It may be several tens of thousands of years or even a hundred thousand years.

A still lower, third horizon of glassy microspherules that occurs in the *Globigerapsis semiinvoluta* zone in the western Pacific and probably in the Indian Ocean has been recognized through high-resolution foraminiferal biostratigraphy (Hut et al. 1986; Keller et al. 1983,1986; Keller 1986). These spherules can be distinguished from the higher upper Eocene spherules on a statistical basis by their chemistry (D'Hondt et al. 1986; Keller et al. 1986). On the basis of the Montanari et al. (1985) recalibration of the late Eocene time scale, the spherule horizon in the *G. semiinvoluta* biozone is very roughly estimated by us as about 0.5 Myr older than the two spherule horizons in the overlying *G. cerroazulensis* zone.

If the ages of the five confirmed horizons of glassy microspherules at ~ 1 Ma and ~ 35 Ma were distributed randomly over the past 35 Myr, the chances that two of them would be deposited in the same 0.1 Myr time interval are about 3%. The joint probability that the age of a third horizon would lie within 0.5 Myr of two horizons separated by 0.1 Myr is about 0.12%. Finally, the joint probability of obtaining both a cluster of three ages like that observed at

~ 35 Ma and a second cluster in which the remaining two ages are separated by less than 0.4 Myr (Table III), is 0.012%. Similar odds for obtaining one tight cluster of three ages and one cluster of two ages are found if we include the nonglassy microspherule horizon at the Cretaceous-Tertiary boundary (as shown at 65 Ma in Fig. 5), and if we consider the ages of six microspherule horizons to be distributed randomly over the last 65 Myr.

The odds of finding the tight clusters at ~ 35 and ~ 1 Ma by chance are impressively low, but the possibility of observational bias should be kept in mind. The three upper Eocene microspherule horizons were discovered, in part, as a result of work initially aimed at tracing out just one microtektite horizon thought to be correlative with the North American tektites. The microtektite horizons of the ~ 1 Ma cluster were found partly by deliberate search for microtektites correlative with previously known tektite strewn fields. Hence, the search for glassy microspherules of impact origin has not been carried out systematically for the last 65 Myr of the stratigraphic column. Keller et al. (1983) reported a few possible glassy microspherules at the Eocene-Oligocene boundary (~ 36 Ma) and in the middle Oligocene (~ 30 Ma). The Eocene-Oligocene boundary objects did not turn out to be glassy microspherules, however, and classification of two objects from the middle-Oligocene has yet to be confirmed. It is hoped that both G. Keller and other micropaleontologists, who will have the opportunity to examine thousands of samples from deep-sea sediments, will look for new horizons of impact microspherules.

Surprising results on the dating of tektites have emerged recently that appear to strengthen the evidence for a tight cluster of impact-event ages near ~ 1 Ma. A great strewn field of tektites that extends from Tasmania to southern China, commonly referred to as the Australasian strewn field, has long been thought to be the product of a single large impact event. New fission-track ages reported by Storzer and Wagner (1980), which appear to be confirmed by new $^{40}Ar/^{39}Ar$ ages by Storzer et al. (1984), suggest that the Australasian field actually consists of two strewn fields of tektites separated in age by about 14×10^4 yr (Table III). Tektites found in Australia (australites) may belong chiefly to the older strewn field, whereas tektites found in Southeast Asia (indochinites and philippinites) may belong chiefly to the younger strewn field. A reexamination of deep-sea cores from the Indian Ocean by Glass (1986) has revealed only one microtektite horizon of about the same age as that reported for Southeast Asian tektites, although a few microtektites were observed at a level that might be correlative with the 0.83 to 0.86 Ma age reported for australites. If the reported age difference between australites and indochinites is firmly demonstrated by further work, two (not one) large tektite-producing impacts on the continents are indicated in the middle Pleistocene. So far, no source crater for these tektites has been identified, although two craters of substantial size and nearly the right age have been found (Table II).

The tight cluster of ages of three microspherule horizons at ~ 35 Ma and the equally tight cluster of ages of microspherule horizons, tektites and impact craters at ~ 1 Ma provide fairly strong circumstantial evidence for comet showers centered at ~ 35 and ~ 1 Ma. Evidently the ~ 1 Ma comet shower has nearly decayed, as the present flux of comets can be explained as the consequence of the background level of stellar perturbation of the outer comet cloud (Oort 1950; Hills 1981) and also by the perturbations due to galactic tidal forces (Morris and Muller 1986; Heisler and Tremaine 1986; chapter by Torbett). The observed frequency distribution of semimajor axes of long-period comets can be accounted for by an equilibrium distribution of comet orbits that results from planetary perturbation of comets from the outer cloud arriving at about the present from the outer cloud flux (Weissman 1978).

The cluster of impact-structure ages and the associated Cretaceous-Tertiary boundary impact event at ~ 65 Ma might also be related to a comet shower, but, on the basis of present evidence, they might also reflect a major catastrophic collision in the asteroid belt. Strong evidence for another comet shower at ~ 65 Ma would be provided if most of the steps in the distributed mass extinction at the Cretaceous-Tertiary boundary were found to coincide with large impacts. We have no evidence, at present, to link the ~ 99 Ma crater-age peak to a comet shower. This peak may just be "shot noise" in our sample of crater ages. The ~ 99 Ma peak is chiefly of interest because it fits the apparent ~ 32 Myr cycle of crater ages rather closely.

Three objections have been raised to the interpretation of two or three comet showers in the observed impact record of the last 100 Myr:

1. The present estimated flux of Earth-crossing asteroids already accounts for the known impact events of this time interval (Grieve et al. 1985);
2. Projectile contamination of investigated impact melt sheets, particularly as revealed by siderophile trace-element abundances, indicates that the impactors were chiefly differentiated asteroids (Grieve et al. 1985; Weissman 1985*c*);
3. No large excursions in the background iridium abundance have been observed in a continuous set of samples from a deep-sea core spanning the interval of 33–67 Ma (Kyte and Wasson 1986).

We examine the merits of each of these objections below.

The present collision rate of Earth-crossing asteroids has been estimated by Shoemaker et al (1979) at about 3.5 asteroids brighter than or equal to absolute visual magnitude 18 per million years. This estimated rate was shown by Shoemaker (1983) to correspond to a probable production on the continents of about four craters ≥ 10 km in diameter per million years. The probable error of the derived asteroid impact cratering rate was estimated as a factor of 2; chief sources of error, of about equal importance, are uncertainties in (1) the Earth-crossing asteroid population, (2) the distribution of albedo and compositional types among the Earth-crossing asteroids, and (3) the crater-scaling relations.

The observed record of large impact events in the past ~ 1 Myr is about that predicted from observations of Earth-crossing asteroids, if the Australasian tektite strewn field represents two events. However, there is an ~ 25% chance that the production of craters ≳ 10 km in diameter by asteroid impact is less than half as great as estimated, and there is a good chance that the identification of large impact events that have occurred on the continents in the last million years is still incomplete. The combined astronomical and geological observations certainly permit a sharp pulse of ~ 1 Myr duration in the impact rate that is at least twice and perhaps several times above background. It is unlikely, on the other hand, that this pulse could have been 10 times above background.

The contribution of the background flux of long period comets must also be considered. The present cratering rate due to comet impact has been variously estimated at about 10% to 50% of the present cratering rate due to asteroid impact (Shoemaker and Wolfe 1982; Weissman 1982*b*). It is not yet clear, however, whether the present comet flux reflects the tail of a pulse. Inclusion of the background flux of comets, in any event, reduces to some extent the plausible amplitude of a comet shower at ~ 1 Ma.

On a longer time scale, Shoemaker et al. (1979), Shoemaker (1983) and Grieve (1984) have suggested that the present flux of Earth-crossing asteroids is consistent with the record of large impact structures in North America, Europe and the USSR for the past hundred or several hundred Myr. It was also recognized, however, that the cratering rate estimated from the present asteroid flux is at least twice the average cratering rate on the Moon over the last 3.3 Gyr.

If a mild comet shower occurred at ~ 1 Ma, one of the consequences would have been an increase in the number of extinct comets in the present Earth-crossing asteroid population. Perhaps half or more of the present Earth-crossing asteroids are either extinct or are dormant, very short period comets (Shoemaker 1984*b*). A moderate to strong comet shower may produce a step increase of a factor of 2 or more in the Earth-crossing asteroid population, which then decays with a characteristic time of a few tens of million years.

In short, not only is there a probable error of a factor of 2 in the estimate of the present cratering rate by asteroid impact, but the present population of Earth crossers may be substantially higher than average, owing to the postulated comet shower at ~ 1 Ma. The integrated contribution of comet showers to the observed record of impact structures of the last 100 Myr could readily amount to about 50%, within the error of estimation of the long-term average population of Earth-crossing asteroids. If comet showers occurred, on the average, about once every 32 Myr, and if each lasted about 1 Myr, the average cratering rate during a shower could be as much as ~ 30 times the background cratering rate.

The composition of the impacting bodies has been estimated from the relative abundances of siderophile trace elements and, in some cases, from the occurrence of taenite or kamacite in the impact melt rocks, for about half the structures listed in Table II. (See Grieve [1982] and Grieve et al. [1985] for a tabulation.) Five of the impactors are classified as iron or iron (?) bodies, one as an iron or achondrite (?), one as an iron (?) or chondrite, one as an achondrite (ureilite), one as a chondrite or achondrite (?), two as chondrites, and one as stone. Of the craters made by these impactors, the ages of nine fall in the clusters that peak at ~ 2, ~ 32, ~ 65 and ~ 99 Ma. From study of the composition of meteoritic dust (Brownlee 1985), most workers think that the nonvolatile component of comets is similar in elemental composition to carbonaceous chondrites. Thus, only four impactors classified in the above list have siderophile element-abundance patterns suggesting that they might have been comet nuclei; two of these do not fall on the crater-age peaks. The impactors at the 1 Myr old craters Zhamanshin and Bosumtwi are both classified as iron, and the impactors at the three structures of the ~ 32 Ma crater-age peak are classified as an achondrite, as an iron or achondrite (?), and as an iron. Hence, the trace-element evidence appears to contravene the comet-shower hypothesis for the origin of the ~ 2 Ma and ~ 32 Ma crater-age peaks and, indirectly, the comet showers at ~ 1 Ma and ~ 35 Ma postulated from the microspherule distribution.

An apparent anomaly in the identification of impactors, however, is that over half are identified chiefly as iron or as differentiated stony meteorite bodies, and another two as possible differentiated bodies. These indicators stand in contrast to the proportions of differentiated meteorites recovered from observed meteorite falls, among which only about 10% are either iron or differentiated stony meteorites (Mason 1962). Moreover, no more than one-quarter to one-half of the bodies that produce very bright meteoritic fireballs are strong enough to reach the ground in the form of recoverable meteorites (Ceplecha and McCrosky 1976; Wetherill and ReVelle 1981). The objects that break up readily in the atmosphere probably are chiefly friable carbonaceous meteorites. Just a few percent of incoming meteoroids are likely to be irons or differentiated meteorites. On the basis of spectrophotometric and broadband photometric observations, no more than 5% to 10% of observed asteroids are likely to be iron objects (Zellner 1979); only two good candidate iron asteroids (Tedesco and Gradie 1986) have been identified among about 30 well-observed Earth-approaching asteroids.

The difficulty with identifying the impacting body from the abundance pattern of siderophile trace elements in impact-melt rocks is that the trace elements, including noble metals that are used principally as a fingerprint for compositional type, may have been fractionated in the shock-melted and partly shock-vaporized material. The observed abundances of noble metals are highly variable in impact-melt rocks and, in our opinion, generally are unreliable guides to the composition of the impacting bodies.

Finally we come to the objection of Kyte and Wasson (1986) that comet showers in the time interval of 33 to 67 Ma are precluded by the observed iridium content in slowly deposited deep-sea sediments. Their objection is based on the assumption that the intensity of a comet shower that might produce mass extinctions is about 200 times the background comet flux. This intensity of shower certainly appears to be precluded by their observations.

The combined astronomical observations of the present Earth-crossing asteroid flux and the geologic record of cratering events suggest that comet showers in the last 100 Myr have been no greater than about 30 times the combined background flux of comet nuclei and asteroids; the "typical" comet shower may be about 10 times background. Kyte and Wasson's observations of a rather broad iridium anomaly near the Cretaceous-Tertiary boundary are entirely consistent with a comet shower of 1 Myr duration peaking at 30 times background, although they attributed the strong anomaly observed at this stratigraphic position to a single event. Other minor peaks that they observed in the iridium distribution in the Eocene could correspond to showers as strong as 10 times the background comet flux. Indeed, Kyte and Wasson found a relatively high abundance of iridium (1 to 2 parts per billion) throughout the middle and upper Eocene, which they attributed to a slow sedimentation rate in the section sampled. In the core that they studied, the general abundance of iridium is so high that the iridium anomaly known to occur in the *G. cerroazulensis* zone is not recognizable. Comet showers whose intensities were 30 times background at ~ 65 Ma and 10 times background at ~ 35 Ma are compatible with the results of their detailed iridium survey.

IV. ASTRONOMICAL CLOCKS

As the four apparent pulses in cratering rate at ~ 2, ~ 35, ~ 65, and ~ 99 Ma appear periodic, it is appropriate to review in some detail the various astronomical mechanisms that have been suggested for periodic modulation of the comet flux. These include:

1. A hypothetical companion star of the Sun on a highly eccentric orbit that perturbs the comet cloud at each perihelion passage (Davis et al. 1984; Whitmire and Jackson 1984);
2. A hypothetical tenth planet (Planet X) that perturbs an inner reservoir of comets when the line of apsides lies close to the line of nodes on the proper plane of the solar system (Whitmire and Matese 1985; Matese and Whitmire 1986; chapter by Matese and Whitmire);
3. Vertical z oscillation of the Sun through the galactic plane, which leads to modulation of the rate of encounter of stars and molecular clouds with the Sun (Rampino and Stothers 1984*a*; chapter by Rampino and Stothers);
4. Passage of the Sun through the galactic spiral arms, which also leads to modulation of the encounter rate of stars and molecular clouds with the Sun (Napier and Clube 1979; Clube and Napier 1982*a*).

The first two of these proposed "astronomical clocks" are speculative, as they involve hypothetical members of the solar system for which there is no direct observational evidence. The second two "clocks" certainly exist, but the amplitude of the periodic or quasi-periodic modulation in the comet flux that they produce is in question.

Solar-Companion Hypothesis

To produce cyclical showers with a period of 30 to 32 Myr, corresponding to the apparent period of pulses in cratering rate, the semimajor axis a_s of an undiscovered solar-companion star must be 97,000 to 101,000 AU. This is approximately the size of the orbit that has long been considered to be the outer bound of the comet cloud (see, e.g., Oort 1950). The outer boundary of the region beyond which a small body would be unbound and would simply drift away from the Sun is an ellipsoid with semiaxes of x = 293,000 AU, y = 196,000 AU and z = 152,000 AU, where x is in the direction toward the galactic center and z is the direction perpendicular to the galactic plane (Antonov and Latyshev 1972). A companion star must have a perihelion distance q_s of ~ 16,000 AU to perturb the inner comet cloud and produce a comet shower, if its mass is ~ 0.1 $M_{\odot}$ (Hills 1984*a*); its eccentricity must be ≳ 0.84 and its aphelion distance Q_s must be ≳ 185,000 AU (for a_s ≈100,000 AU). The eccentricity could be much smaller only if the mass of the companion is much closer to the solar mass. If the mass is 0.2 $M_{\odot}$, the perihelion distance required to produce a comet shower is ≲ 30,000 AU and the aphelion must be ≳ 170,000 AU. Torbett and Smoluchowski (1984) and Torbett (see his chapter) have shown that, if the inclination of the orbit of the companion star to the galactic plane exceeds about 30°, a small companion capable of producing comet showers would become unbound over solar system time by the action of the galactic tidal forces alone.

At aphelion distances of 170,000 to 190,000 AU, a companion star would be very weakly bound to the Sun, even if the orbital inclination lay in the stable region. Perturbations by passing stars and molecular clouds would tend to detach the companion over a period of time shorter than solar system time. Therefore, it comes as no surprise that, although binary stars with separations up to ~ 20,000 AU are fairly common (Bahcall and Soneira 1981; Latham et al. 1984), none has been recognized with a separation remotely approaching 100,000 AU. On strictly empirical grounds, it appears unlikely that the Sun is accompanied by a star with the semimajor axis and eccentricity required to produce cyclical comet showers with a period of 30 to 32 Myr.

In order to evaluate the probability that a distant solar companion exists, we have carried out a series of Monte Carlo calculations that began with the orbital evolution of the companion at various distances from the Sun. We treated the companion simply as a very large planet (i.e., a body having a small mass compared with the mass of the Sun). We studied two different cases, one in which perturbations by passing stars alone were considered, and one which also included perturbations by giant molecular clouds.

For the case involving perturbations by passing stars alone, 100 trials were run at each of the following starting semimajor axes: 10,000, 20,000, 30,000, 40,000, 50,000, 70,000, 80,000, 87,764 and 100,000 AU. Initial eccentricity e_0 of the solar companion was taken as 0 and its orbital plane was taken as initially coincident with the proper plane of the solar system as determined from the known planets. A mass distribution for passing stars down to 0.1 $M_\odot$ was adopted from the present mass distribution in the solar neighborhood as estimated by Miller and Scalo (1979). A total mass density for observable stars in the solar neighborhood of 0.1 $M_\odot$ pc^{-3} (see reviews by Krisciunas [1977] and Bahcall [1984*a*]) and a uniform speed of 20 km s^{-1} for all stars with respect to the Sun, appropriate for the weighted average of various classes of stars (Delhaye 1965), were adopted. Although a more realistic distribution of speed, dependent on stellar mass, could have been used, the assumption of uniform speed is considered conservative, in that it eliminates rare strong perturbations due to slow encounters. The motion of the companion about the Sun was taken to be Keplerian until perturbed by a passing star. Perturbations were calculated by the impulse approximation; impulses were derived from the approximate formula used by Oort (1950) and determined for the time of closest approach of the star to the Sun or to the solar companion. Corrections were applied for the finite durations of the perturbations, as derived by Hut and Tremaine (1985). New orbital elements after each perturbation were computed on the basis of Öpik's (1951) equations, and the motion after each perturbation was again considered Keplerian. The motion of the companion was followed until the orbit passed beyond the envelope of stability or for 4.5 Gyr. The results are illustrated in Fig. 7.

In the case of perturbations by passing stars alone, the companion star survived over solar system time (4.5 Gyr) in 91% of the trials, when started with a semimajor axis a_0 of 10,000 AU. The fraction surviving for 4.5 Gyr dropped rapidly with increasing a_0, however. At a_0 = 50,000 AU, the fraction dropped to 25%; at a_0 = 100,000 AU, it dropped to 4%. In most cases of survival with large initial orbits, we found that the final semimajor axes a_f were much smaller than a_0. Only 8% of the trials started at 50,000 AU yielded survivors with a_f larger than the starting orbit, and the 100 trials started at 100,000 AU yielded only one survivor with $a_f \geq$ 50,000 AU. For $a_f \geq$ 50,000 AU, a maximum of 12% survivors was found at a_0 = 40,000 AU.

It could be argued that we used too large a flux for the passing stars in our Monte Carlo calculations, as the Sun is now near the galactic plane and the present flux may be near a maximum. If the Sun had a much larger *z* oscillation in the past, the mean flux of stars might have been lower by about a factor of 2. On the other hand, we neglected objects smaller than 0.1 $M_\odot$, which might account for about half the local mass density of the Galaxy; the whole mass is now estimated to be about 0.19 $M_\odot$ pc^{-3} (Bahcall 1984*a*,1986). Moreover, passing stars are not the principal cause of unbinding of wide binary systems. The much more massive giant molecular clouds, with masses up to ~ 10^6 $M_\odot$, are more effective than stars in detaching distant companion stars over solar system time.

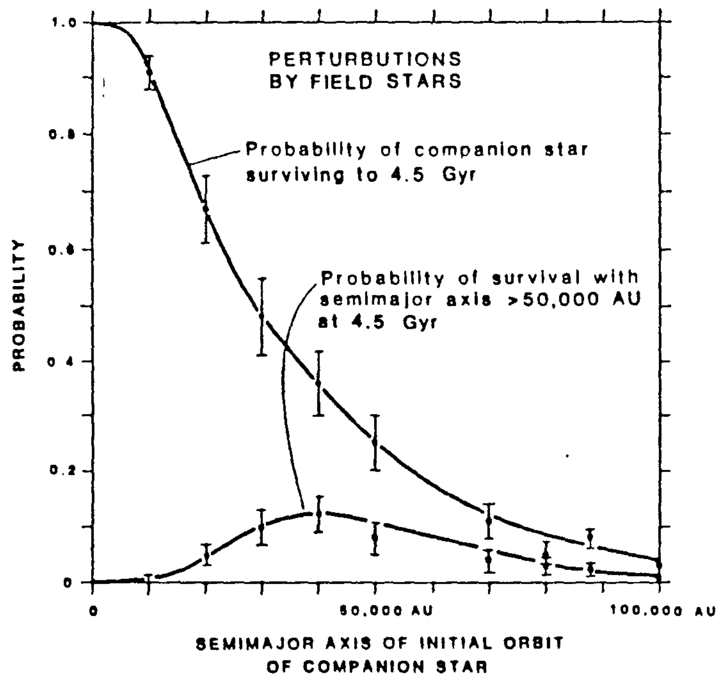

Fig. 7. Probability of survival for 4.5 Gyr of a solar-companion star whose orbit is subject to impulsive perturbations only by passing field stars in the Galaxy. The upper curve shows total probability of survival; the lower curve shows combined probability of surviving and also having a semimajor axis > 50,000 AU at 4.5 Gyr from the beginning of the perturbation history. Estimates of probability are based on a Monte Carlo procedure described in the text. All Monte Carlo runs begin with the companion star in a circular orbit that is in the proper plane of the solar system as determined from the observed planets.

In the second series of Monte Carlo runs, we added perturbations by giant molecular clouds to the perturbations by stars. A smooth mass-frequency distribution of molecular clouds, from 10^3 $M_\odot$ to 10^6 $M_\odot$, fitted to a distribution suggested by van den Berg (1982), was adopted; the mean density of molecular clouds through the region traversed by the Sun was taken as 0.0128 $M_\odot$ pc^{-3}. This mean density corresponds to a density at the galactic midplane of 0.026 $M_\odot$ pc^{-3}, which is nearly the same as that adopted by Hut and Tremaine (1985) and somewhat lower than that estimated by Sanders et al. (1984). The perturbations by the molecular clouds were also modeled by the impulse approximation, with corrections for the durations of the perturbations and for the finite sizes of the giant molecular clouds derived from the work of Hut and Tremaine (1985). Trials were started, as before, with orbits for the hypothetical solar companion at $e_0 = 0$ and the orbit plane in the proper plane of the solar system. At $a_0 = 100{,}000$ AU, there were no survivors out of 100 trials; the maximum time to detachment of the companion star was ~ 1.7 Gyr, and the mean time was 196 Myr. Giant molecular clouds accounted for about one-third of the total perturbations and were responsible for three-fourths of the final perturbations in which the companion was lost. Trials were also run at a_0 = 10,000, 20,000, 30,000, 40,000 and 87,764 AU. The fractions surviving were 56% at 10,000 AU, 22% at 20,000 AU, 9% at 30,000 AU and 3% at 40,000 AU (Fig. 8). It can be fairly readily understood from these results why no binary star systems have been discovered with separations much greater than 20,000 AU (see also Bahcall et al. 1985). A maximum of ~ 1% survivors with a_f > 50,000 AU at 4.5 Gyr was obtained in the range a_0 = 10,000 to 30,000 AU.

After we presented these results at the conference *The Galaxy and the Solar System*, Tucson, Jan. 1985, a paper by Weinberg et al. (1986) appeared that gave an analysis of the stability of wide binaries based on a different method of calculation and somewhat different canonical values of the number

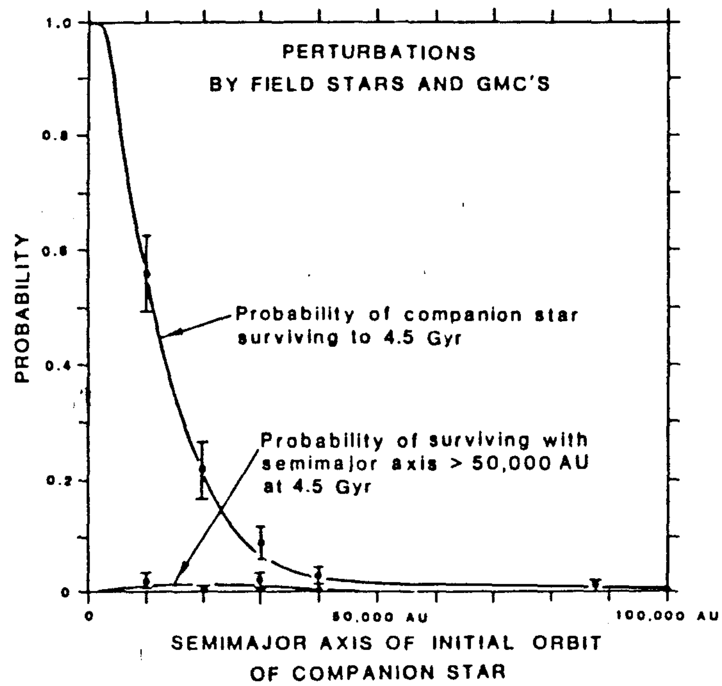

Fig. 8. Probability of survival for 4.5 Gyr of a solar-companion star whose orbit is subject to perturbations both by field stars and molecular clouds. The upper curve shows total probability of survival; the lower curve shows combined probability of surviving and also having a semi-major axis > 50,000 AU at 4.5 Gyr from the beginning of the perturbation history. Estimates of probability are based on a Monte Carlo procedure described in the text. All Monte Carlo runs began with the companion star in a circular orbit that is in the proper plane of the solar system as determined from the observed planets.

density, masses and velocities of the perturbing bodies. They found even shorter lifetimes for wide binaries than ours.

We conclude that the odds are no greater than $\sim$ 1% that the Sun has a companion star with a semimajor axis in the range necessary for the production of comet showers with any period > 11 Myr (a >50,000 AU). Indeed, 1% may be a generous upper bound. Moreover, to produce comet showers with a period of 30 to 32 Myr, the solar companion must also have an eccentricity of $\gtrsim 0.7$, if its mass is relatively large, and $\gtrsim 0.9$ if its mass is small. There is a $\lesssim 50\%$ chance that the eccentricity of the companion is $\gtrsim 0.7$, and $\lesssim 20\%$ that the eccentricity is $\gtrsim 0.9$ (see, e.g., Hills 1981, for the theoretical frequency distribution of eccentricities). Finally, the orbit of the companion must be fairly stable for $\sim$ 100 Myr in order to produce the apparent periodicity observed in the crater ages. From our Monte Carlo trials at a_0 = 100,000 AU, we found that there is a chance of < 50% that the orbit remains sufficiently stable over 100 Myr. When giant molecular cloud perturbations are included, the solar companion is lost before 100 Myr in $\sim$ 40% of the trials. The overall odds that a companion star produces comet showers with a period of about 30 to 32 Myr appear to be no better than about 1 in 1,000.

V. PLANET X HYPOTHESIS

Whitmire and Matese (1985) suggested that an undiscovered tenth planet orbiting in the region beyond Pluto might produce comet showers in the vicinity of the Earth with a very stable frequency. In their hypothesis, Planet X has a substantial orbital eccentricity e_x and inclination i_x; it revolves within a gap, cleared by the planet, in a thin disk of comet nuclei. Showers of comets occur when the perihelion and aphelion of Planet X pass near the edges of the gap in the plane of the comet disk, as a result of the steady advance of the argument of perihelion ω_x. Two passages of the aphelion and perihelion through the plane of the comet disk occur during every 360° advance of ω_x. The period T_ω is determined chiefly by the size of the major axis of Planet X, $2a_x$, which precesses under the well-known perturbing influence of the other planets. From the formula adopted by Whitmire and Matese (1985), the required value of a_x is about 105 AU for $0.5\,T_\omega = 31$ Myr, on the assumption that $e_x \approx 0.25$ and $i_x \approx 15°$; T_ω is relatively insensitive to moderate variations in e_x and i_x.

For comet showers to occur, it is essential that Planet X clear a gap or greatly reduce the areal density of comets in the region between the perihelion distance q_x and aphelion distance Q_x of the planet. Moreover, the edge of the gap or depleted region must be fairly sharply defined. The comets might either be lost entirely from the neighborhood of Planet X or be piled up just sunward of q_x and beyond Q_x (Matese and Whitmire 1986). Comets in the relatively undepleted disk on both sides of the gap are envisioned as diffusing toward the gap edge as a result either of perturbations by large comet nuclei embedded in the comet disk (Whitmire and Matese 1985) or of the intermediate-range perturbing influence of Planet X itself (Matese and Whitmire 1986). The origin of the gap is not discussed in detail by Whitmire and Matese (1985), although it is treated indirectly by Matese and Whitmire (1986). We consider the putative gap to be the Achilles heel of this intriguing hypothesis.

In order to test whether a gap is a stable feature of the Planet X-comet disk system postulated by Whitmire and Matese, we conducted a number of Monte Carlo simulations of the system. Trial runs were made for various assumed values of i_x and for the mass of the planet m_x with 506 comets each, starting with comet orbits near the aphelion and perihelion of Planet X. All comets were initially assigned an eccentricity e_c of 0.1 and an inclination i_c of 0.05 radians (2°865) to the central plane of the comet disk (assumed to be the proper plane). Comet semimajor axes a_c were chosen near q_x and Q_x such that all comets could encounter Planet X. The semimajor axes were distributed to simulate steep diffusion gradients at the gap edges. Cases were investigated for $i_x = 5°$, 15° and 45° and corresponding values for a_x = 106.0, 104.5 and 80.0 AU; e_x was assumed to be 0.25 when $i_x = 5°$, 15°; $e_x = 0.3$ when i_x = 45° (cf. canonical value of $e_x = 0.3$ adopted by Matese and Whitmire 1986). Masses of 5 $m_\oplus$ and 10 $m_\oplus$ were adopted for Planet X (cf. 5 $m_\oplus$ adopted by Matese and Whitmire 1986), and a few runs were made with $m_x = 1\ m_\oplus$.

The evolution of the comet orbits was followed by a Monte Carlo procedure derived from that described by Arnold (1965), which we have used extensively to investigate the dynamical history of the Uranus-Neptune planetesimal swarm (Shoemaker and Wolfe 1984). Perturbations due to encounters with Planet X and the known planets, as well as the times between encounters, were based on Öpik's (1976) equations for single encounters; changes in orbit due to all encounters within Öpik's (1951) radius of action were calculated for each comet. Perturbations due to encounters of stars with the solar system were also included in the Monte Carlo code for all orbits that started with or evolved to semimajor axes in excess of 100 AU. The effective impulses due to stellar encounters were calculated as described above in our investigation of the hypothetical solar-companion star. In general, the contribution of stellar perturbations was very small, except when the orbits evolved to large size ($a_c > 10^3$ AU). The history of each comet orbit was followed until the comet was ejected from the solar system or until it collided with a planet or the Sun; if neither event occurred, the orbit was followed for 4.5 Gyr. A statistical summary of the results is given in Table IV.

Early trials quickly showed that a planet of 1 $m_\oplus$ to 5 $m_\oplus$ would be ineffective in clearing a gap in the comet disk at any distance appropriate for the Planet X hypothesis. Therefore, we concentrated our investigation on the effects of a 10 $m_\oplus$ planet, in order to elucidate the general pattern of orbital evolution of comets in this region. Even a 10 $m_\oplus$ planet does not clear a gap, although it can reduce significantly the number of comets in the region of close encounters in the cases that we studied, the fraction of comets remaining in the neighborhood of Planet X after 4.5 Gyr ranged from 68% to 82%, for Monte Carlo runs in which $i_x = 5°$, 15°; the fraction remaining in runs with i_x

TABLE IV

Statistical Summary of Results from Monte Carlo Simulations of the Orbital History of Comets in the Neighborhood of Planet X

Parameters of Planet X			Fraction of Comets Surviving in Neighborhood of Planet X After 4.5 Gyr		Mean Semimajor Axes of Comet Orbits				Mean Eccentricities of Comet Orbits			
Mass	Orbital Inclination	Semimajor Axis	Comets Initially Near q_x	Comets Initially Near Q_x	Comets Initially Near Perihelion of Planet X (q_x)		Comets Initially Near Aphelion of Planet X (Q_x)		Comets Initially Near Perihelion of Planet X (q_x)		Comets Initially Near Aphelion of Planet X (Q_x)	
	(deg)	(AU)	(%)	(%)	Initial Mean Semimajor axis	Geometric Mean Semimajor Axis After 4.5 Gyr	Initial Mean Semimajor Axis	Geometric Mean Semimajor Axis After 4.5 Gyr	Initial Eccentricity	Mean Eccentricity After 4.5 Gyr	Initial Eccentricity	Mean Eccentricity After 4.5 Gyr
					AU	AU	AU	AU				
5 $m_\oplus$	15	104.5	89.4		72.00	163.15			0.100	0.445		
10 $m_\oplus$	5	106.0	67.79	70.5	74.17	412.10	145.46	360.00	0.100	0.652	0.100	0.619
	15	104.5	72.13	83.2	73.15	279.90	143.37	225.32	0.100	0.570	0.100	0.529
	45		22.7	96.6	54.36	475.77	113.80	168.35	0.100	0.710	0.100	0.406
		{ 80.0	44.6	81.8	62.23	349.70	89.77	198.38	0.100	0.656	0.100	0.509

Parameters of Planet X			Mean Inclinations of Comet Orbits				Ratio of Comets Perturbed Directly to Jupiter- and Saturn-Crossing Orbits to Total Comets Lost Out of 506 Trial Runs	
Mass	Orbital Incli-nation	Semi-major axis	Comets Initially Near Perihelion of Planet X (q_x)		Comets Initially Near Aphelion of Planet X (Q_x)		Comets Initially Near Perihelion of Planet X (q_x)	Comets Initially Near Aphelion of Planet X (Q_x)
	(deg)	(AU)	Initial Incli-nation	Mean Incli-nation After 4.5 Gyr	Initial Incli-nation	Mean Incli-nation After 4.5 Gyr		
			(deg)	(deg)	(deg)	(deg)		
5 $m_\oplus$	15	104.5	2.865	7.71				
10 $m_\oplus$	5	106.0	2.865	17.07	2.87	14.45	53/61	74/77
	15	104.5	2.865	12.79	2.87	9.98	65/76	28/57
	45	80.0	2.865	23.81	2.87	8.33	250/269	8/8
			2.865	18.78	2.87	10.46	162/172	56/59

= 45° ranged from 23% to 97% (Table IV). Comets removed from the strong-encounter region were not piled up on both sides of the depleted region, as suggested by Matese and Whitmire (1986). Instead, nearly 90% of the comets removed from the neighborhood of Planet X were perturbed directly to Saturn- and Jupiter-crossing orbits and were ejected from the solar system. The remainder were lost chiefly by ejection due to encounters with Neptune or Uranus.

In every set of Monte Carlo runs, the semimajor axes, eccentricities, and inclinations of comets remaining in the neighborhood of Planet X tended, on average, to increase with time, and the distribution of all three orbital elements became widely dispersed. The geometric mean of the semimajor axes generally increased to several hundred AU, the mean eccentricity increased to about 0.5 to 0.7, and the mean inclination to about 10° to 19°. Except in the cases of comets near q_x and Q_x when i_x = 45°, the trends and the amounts of orbital evolution were relatively insensitive to the starting orbits of the comets. In most cases, the final distribution of orbits for comets starting near the perihelion distance of Planet X, q_x, was not statistically discriminable from the final distribution for comets starting near the aphelion distance Q_x.

Our results show that, while the number density of comets in the neighborhood of Planet X can be reduced if the planet is very massive, and while the probability of encounter with Planet X for the remaining comets is also reduced as a result of dispersion of their orbital elements, it is impossible for Planet X to form a gap with sharp edges. In fact, if a sharp-edged gap in the comet disk were formed initially by some other mechanism, Planet X would disperse the comets near the gap's edges. If comets diffused toward the edges, the gradients of comet density near the original edges would be low at the present time, and the gap would be partly filled with the dispersed comets. If no gap were formed by other, unspecified mechanisms, a 10 $m_\oplus$ Planet X with high inclination would significantly deplete the density of comets near q_x. The result would be that the minimum rate of comet perturbation would now occur when the apsides lie near the central plane of the comet disk. This is precisely the opposite effect from that predicted by Whitmire and Matese.

Because the perturbations by Planet X would tend to fill a sharp-edged gap, rather than create one, and would smooth out the edges, we consider it very unlikely that an undiscovered planet is responsible for comet showers. On the other hand, if a relatively massive planet exists in the region beyond Pluto, and if this region is fairly densely populated with comets, there is no question that this planet could perturb comets fairly efficiently into Jupiter-crossing orbits. Therefore, a tenth planet could contribute to the capture of Jupiter-family comets and account for part of the background population of these comets, as suggested by Matese and Whitmire (1986).

There are three principal reasons, however, for doubting the existence of a relatively massive (2 $m_\oplus$ to 5 $m_\oplus$) planet beyond the orbit of Pluto. First of all, the reported residuals in the motion of Uranus and Neptune used to deduce the existence of Planet X (Rawlins and Hammerton 1973) may be spurious. We now know the present position and motion of Uranus with great accuracy as a result of the Voyager 2 encounter; comparison of the position and motion of Uranus derived from spacecraft-tracking data with those derived from conventional astrometric observations reveals systematic errors in the relatively recent astrometry (M. Standish, personal communication, 1986). In our judgment, the reported residuals in the motion of both Uranus and Neptune may be due largely or entirely to systematic errors of both the old as well as the more recent astrometric measurements (see also the chapter by Anderson and Standish).

Secondly, a planet whose mass is in the range 2 $m_\oplus$ to 5 $m_\oplus$ probably would have an apparent *B* magnitude in the range 13 to 15 (cf. Matese and Whitmire 1986). This magnitude is significantly brighter than the conservatively estimated limit of completeness of the survey for additional planets conducted by Tombaugh (1961). If a planet as bright as magnitude 13 to 15 exists, its orbital inclination must be high and it must have been hiding in the southern skies below the declination limits of Tombaugh's survey.

Finally, the time scale of planetary accretion at distances beyond the aphelion of Pluto is long in comparison with solar system time. It is unlikely that a planet as massive as $\gtrsim 1$ $m_\oplus$ could have formed in this region. It is also unlikely that a planet of large mass (i.e., ~ 10 $m_\oplus$) could have been deflected into this region by encounter with Neptune (cf. Harrington and Van Flandern 1979) without leaving Neptune in a much less regular orbit than what we observe today. On the other hand, it is entirely plausible that planets about the size of Pluto remain to be found at distances of 50 to 100 AU; systematic searches for faint distant planets are appropriate and timely (Kowal 1979; C. S. Shoemaker, unpublished proposal).

VI. OSCILLATION OF THE SUN PERPENDICULAR TO THE GALACTIC PLANE

The hypothesis of Rampino and Stothers (1984*a*) that the vertical *z* oscillation of the Sun through the galactic plane leads to periodicity of comet showers has two attractive features. Both the period and phase of the cyclical comet showers predicted by this hypothesis fit the apparent pulses in cratering rate over the last 100 Myr. The Sun's last crossing of the galactic plane occurred at about the time of the crater-age peak centered at ~ 2 Ma. The height of the Sun above the galactic plane $z_\odot$ is variously estimated at 8 ± 12 pc, from observations of H I clouds, to 20 to 30 pc, from the distribution of young stars and star clusters (Stothers 1986). As the Sun's *z* component of velocity $Z_\odot$ is fairly well determined at about 8.6 ± 1 km s^{-1}, (8.8 ± 1 pc yr^{-1}) (Stothers 1986), the last plane crossing probably occurred in the last ~ 3 Myr, perhaps at 1 ± 1 Ma, if H I observations provide the best frame of reference for $z_\odot$ (see also Bahcall and Bahcall 1985). Taking Bahcall's (1984*a*) latest estimate of $0.185 \pm 0.02\ m_{\odot}\ pc^{-3}$ for the local mass density at the galactic plane $\rho_{\odot}$, we can roughly estimate the half period $P_{1/2}$ of the z oscillation of the Sun from the formula for a harmonic oscillator:

$$P_{1/2} = (\pi/4G\rho_{\odot})^{1/2} = 30.7 \pm 0.2 \text{ Myr}. \quad (1)$$

This period matches very closely the best-fit period derived from the ages of impact structures over the last 165 Myr and the best-fit period for impact glass, microspherule horizons and iridium anomalies. Bahcall and Bahcall (1985) have evaluated the period and height of the Sun's oscillation on the basis of a variety of models of the vertical distribution of mass in the galactic disk and found periods ranging from ~ 26 Myr to ~ 36 Myr. The most conventional model, based on approximately equal amounts of unobserved and observed material, yields periods of 30.8 to 32.1 Myr, which again match very closely the period obtained from the dates of terrestrial impact events. Perturbations of the Sun's motion due to encounters with a massive object typically produce a jitter in the phase of oscillation of about 6 to 9%.

The principal difficulty with the hypothesis of Rampino and Stothers is that stars and molecular clouds, whose encounters with the Sun produce comet showers, are not sharply concentrated at the galactic plane. The scale height of observable stars, at the present galactocentric radius of the Sun, is variously estimated at 46 pc to 57 pc; somewhat similar estimates are made for the vertical distribution of molecular clouds (see Stothers [1986] for a review). An amplitude of z excursion of the Sun from the galactic plane z_{max} consistent with the values of $z_{\odot}$, $Z_{\odot}$ and $P_{1/2}$ used above can be roughly estimated from the harmonic oscillation formula by

$$z_{max} = (z_{\odot}^2 + P_{1/2}^2 Z_{\odot}^2/\pi^2)^{1/2} = 86 \pm 4 \text{ pc}. \quad (2)$$

As shown by Bahcall and Bahcall (1985), however, this formula tends to overestimate z_{max} by about 5% to 30%, depending on the actual vertical distribution of mass in the galactic disk. For the most conventional model, they find $z_{max} \simeq 70$ pc. As z_{max} is comparable to or possibly slightly greater than the probable scale height of most perturbing bodies, a fairly strong fluctuation should occur in the probability of occurrence of a comet shower over a half cycle of z oscillation. Depending on the model of vertical mass distribution, the present amplitude of the variation probably is about a factor of 2 to 5. The Sun passes rather quickly through the region of highest density of perturbing bodies, however, so that a substantial fraction of comet showers should occur at times when the Sun is far from the galactic plane.

Stothers (1986) has shown that the periodicity of comet showers should be detectable in the existing terrestrial impact record for the last ~ 600 Myr, provided that the z distribution of perturbing bodies in the galactic disk is not dominated by a dispersed component near z_{max}. For a much shorter interval of time, the detection of periodicity is problematical. To first order, the distribution in time of the last 4 comet showers should be more nearly random than periodic.

In the limiting favorable case that the distribution of all the mass near the present galactocentric radius of the Sun is distributed with a scale height of 50 ± 5 pc, Stothers (1986) found that about 74% of the encounters of perturbing bodies with the Sun should occur during the 50% of the cycle of z oscillation when the Sun is closest to the galactic midplane. Under these conditions, there are *a priori* probabilities of ~ 40% that a comet shower occurred within ± 0.5 $P_{1/2}$ of each of the last 3 midplane crossings and ~ 30% that comet showers occurred within ± 0.5 $P_{1/2}$ of the last 4 crossings (assuming unit probability of a comet shower during each one-half cycle of z oscillation). The apparent pulses in cratering rate at ~ 2, ~ 35, ~ 65 and ~ 99 Ma are, however, much closer to the estimated times of midplane crossing than ± 0.5 $P_{1/2}$. Deviations in time from perfectly periodic crossings corresponding to the harmonic oscillator solution for $z_{\odot}$ = 8 pc, $Z_{\odot}$ = 8.6 km s^{-1} and $P_{1/2}$ = 30.7 Myr are no greater than ~ 0.2 $P_{1/2}$. The probability of a shower-producing perturbation occurring within ± 0.2 $P_{1/2}$ of the midplane crossing is only ~ 0.3. Hence the *a priori* odds that the last three comet showers should have occurred this close to the estimated time of crossing are no greater than ~ $(0.3)^3$ ≃ 3%; the odds that the last 4 showers occurred this close to the midplane crossing are ~ 1%. If periodicity of large body impact on Earth is attributed largely or entirely to the modulation of comet showers by the z oscillation of the Sun, it is difficult to escape the conclusion that the near coincidence of the last 4 apparent pulses in cratering rate with a likely sequence of times of galactic midplane crossings is an improbable statistical fluke.

Thaddeus and Chanan (1985) have analyzed the probability of detecting periodicity in the terrestrial cratering record produced solely by perturbations of the comet cloud by molecular clouds. They found the scale height of molecular clouds to be somewhat greater than z_{max}, and they concluded that observations of the impact effects of more than 300 comet showers would be required to detect even a relatively modest periodic signal. On independent grounds, however, it is unlikely that molecular clouds are responsible for the apparent 30 to 32 Myr periodicity in the impact record. Encounters with molecular clouds are insufficiently frequent, and long-range encounters with giant molecular clouds are ineffective in perturbing the inner comet reservoir, where comet showers must originate. Most sharply defined comet showers (half life ~ 1 Myr) must be produced chiefly by stellar perturbations of the inner comet reservoir.

VII. PASSAGE OF THE SUN THROUGH THE GALACTIC SPIRAL ARMS

It has been realized for many years that the Sun must travel through the spiral arms of the Galaxy; in an extended series of papers, W. M. Napier and

S. V. M. Clube have discussed how the encounter of the Sun with a giant molecular cloud might produce a strong comet shower. In most of their papers, they have argued that the Oort cloud of comets would be stripped from the Sun during a giant molecular cloud encounter and that there would be a shower of comets derived from the molecular cloud. They have further pointed out that the probability of encounter with a molecular cloud is enhanced during passage through a galactic spiral arm. As spiral-arm passages are quasi-periodic, the comet showers produced would be quasi-periodic also (see, e.g., Napier and Clube 1979; Clube and Napier 1982*a*). Recent investigations show that the Sun's comet cloud is fairly stable against stripping by giant molecular cloud encounters (Hut and Tremaine 1985), a result that is confirmed by our study of the stability of a solar-companion star given above. The outer bound of the comet cloud is established primarily by molecular cloud encounters; comets stripped from the outer edge probably are replaced by outward diffusion of comets from the massive inner part of the cloud. The vast majority of comets that have entered the inner solar system probably are original members of the system and were derived from the cloud of comets that has remained bound to the Sun. Nevertheless, the quasi-periodic passage of the Sun through the galactic spiral arms almost surely modulates, to some extent, the flux of comets at the Earth.

The spiral arms of the Galaxy are controlled by waves of stellar density that revolve about the galactic center at about half the rate of revolution of the stars themselves at the present galactocentric distance of the Sun (Lin et al. 1969). There is some debate as to whether our Galaxy has two spiral arms, as observed in most other spiral galaxies and assumed by Lin and his coworkers, or whether it has four spiral arms (Blitz et al. 1983). The average period between spiral-arm passages of the Sun is approximately equal either to half the galactic year (~125 Myr), or to one-quarter of the galactic year. As both the orbit of the Sun and the spiral arms are somewhat irregular, the time between spiral-arm passages should also be somewhat irregular. In any event, the mean period is about two to four times greater than the apparent period of pulses in terrestrial cratering.

The increase in encounter rate with stars during spiral-arm passages probably is on the order of 5% to 10% (cf. Lin et al. 1969). Molecular clouds may be somewhat more concentrated in the arms, where the clouds are evidently shock compressed. This compression accounts for the birth of massive young stars that make the arms visible (Shu et al. 1972). It is certain that the rate of encounter with these stars is highest in the arms, which increases the rate of perturbation of the inner comet cloud during passage through an arm. Overall, the probability of perturbation of the inner comet cloud may increase by about 10% during spiral-arm passages. The resulting quasi-periodic modulation of the terrestrial cratering rate would be detectable only with a very long and much more complete record of impact structures than is available to us now.

VIII. SUMMARY

The formation of large impact craters in the last 220 Myr appears to have been moderately cyclical, with a best-fit period of 30 to 31 Myr; four apparent pulses in the cratering rate, broadly centered at ~ 2, ~ 35, ~ 65 and ~ 99 Ma, are fairly strongly cyclical, with a best-fit period of 32 Myr. Sharp pulses of impact events at ~ 1 Ma and ~ 35 Ma are indicated by strewn fields of impact microspherules. The period and phase of the impact-event cycles match fairly closely the best-fit cycle obtained from strong well-dated mass extinctions; impact pulses at ~ 35 Ma and ~ 65 Ma, in particular, are correlated with strong stepwise mass extinctions. The sharp pulses of impact events are best explained by comet showers stimulated by close encounters of stars or molecular clouds with the Sun.

Neither the solar-companion star hypothesis nor the Planet X hypothesis appears to offer a likely mechanism for producing periodic comet showers. While the existence of a star revolving about the Sun on an orbit of the size, eccentricity and short-term (~100 Myr) stability required to produce the four apparent pulses in impact rate cannot be disproved, the odds that a star with the required orbit exists appear to be no better than 1:1000. An undiscovered tenth planet whose apsides precess with respect to the node with a period of 30 to 32 Myr might well exist, but we have found that such a planet, even if it is as massive as 10 $m_{\oplus}$, would not clear a sharp-edged gap in a thin disk of comet nuclei. Therefore, the postulated Planet X cannot produce detectably cyclical comet showers.

Oscillation of the Sun normal to the galactic plane appears to have very close to the right frequency and phase to explain the apparent pulses of impact events in the last 100 Myr. However, the correlation in time between apparent impact pulses and the last four galactic midplane crossings of the Sun, calculated on the basis of Bahcall's (1984*a*) estimate of the mass density in the solar neighborhood, is much stronger than can be expected from any plausible scale heights of stars and molecular clouds above the galactic plane. The *a priori* odds of finding a correlation as high as that observed are ~ 3% for the last three apparent pulses and ~ 1% for the last four.

Quasi-periodic passage of the Sun through the galactic spiral arms probably has resulted in very weak (~10%) modulation of the comet flux. If the Galaxy has four arms (Blitz et al. 1983), the mean period between passages of the Sun through the arms is close to twice the period of passages through the galactic plane and might lead to reinforcement of the modulation due to z oscillation, provided the passages are approximately in phase.

To sum up, the z motion of the Sun has probably resulted in periodic modulation of the comet flux at the orbit of the Earth sufficiently strong that the period should be detectable in the long term (Phanerozoic) cratering record. This is especially true if, during most of the Phanerozoic, z_{max} were closer to the average height expected for a star of the Sun's mass and age. The very good fit of the last four apparent impact pulses evidently is a statistical fluke. The odds of occurrence of such a fluke, on the other hand, are at least an order of magnitude better than the odds that a solar companion is responsible for the impact pulses. Most comet showers are generated by close passages of stars, and the estimated strength and frequency of possible showers in the last 100 Myr is roughly consistent with the estimated flux of stars in the solar neighborhood.

If most strong mass extinctions are related to comet showers, a periodicity probably should also be detectable in mass extinctions over Phanerozoic time. However, the present chronometric control for the geological time scale is inadequate to demonstrate periodicity of the known mass extinctions. A crucial direction for future research is to identify and accurately date a much larger fraction of the terrestrial impact events that have occurred in the last half-billion years and to determine accurately the correlation between these events and the recognized biological crises. If comet showers have been the primary trigger for mass extinctions, most mass extinctions probably have occurred in discrete steps distributed over intervals of no more than a few million years. Therefore, the detailed history of each mass extinction should be examined by means of intensive stratigraphic studies. Evidence for large impact events should be looked for both at the stratigraphic position of each extinction step and in the general stratigraphic interval of the mass extinctions.

Acknowledgments. It is a pleasure to acknowledge detailed discussions, correspondence and exchange of information over the past few years with L. Alvarez, W. Alvarez, F. Asaro, J. Bahcall, V. Clube, S. D'Hondt, W. Glass, R. Grieve, J. Hills, P. Hut, G. Izett, A. Jackson, E. Kauffman, G. Keller, F. Kyte, J. Matese, S. Montanari, R. Muller, C. Orth, M. Rampino, D. Raup, J. Sepkoski, R. Smoluchowski, M. Standish, S. Stanley, D. Storzer, R. Stothers, M. Torbett, J. Wasson, P. Weissman and D. Whitmire. We thank D. Raup, in particular, for very helpful critical review of an early draft of the manuscript. Finally, we are indebted to D. Weir, S. Bounds, and C. Shoemaker, without whose special help the manuscript could not have been brought to a satisfactory editorial state in time, and to M. S. Matthews and R. Smoluchowski for their encouragement and patience.